https://doi.org/10.1016/j.enggeo.2023.107005
This is the Pre-Published Version.

Effects of Temperature on the Time-Dependent Compression and Shear Behaviour of a Soft Marine Clayey Soil

by
Ze-Jian Chen
Postdoctoral fellow, Department of Civil and Environmental Engineering, The Hong Kong Polytechnic University, Hong Kong, China
ORCID ID: 0000-0001-7855-6234
Email: zejian.chen@polyu.edu.hk

Run-Dong Zhao
Research Assistant, Department of Civil and Environmental Engineering, The Hong Kong Polytechnic University, Hong Kong, China
Email: rundong.zhao@connect.polyu.hk

Wen-Bo Chen (Corresponding author)
Research Assistant Professor, Department of Civil and Environmental Engineering, The Hong Kong Polytechnic University, Hong Kong, China
ORCID ID: 0000-0002-4145-5445
Email: wb.chen@polyu.edu.hk

Pei-Chen Wu
Research Assistant Professor, Department of Civil and Environmental Engineering, The Hong Kong Polytechnic University, Hong Kong, China
OCRID: 0000-0001-7900-3703
Email: elvis.wu@polyu.edu.hk

Jian-Hua Yin
1: Chair Professor, Department of Civil and Environmental Engineering
2: Research Institute for Land and Space
The Hong Kong Polytechnic University, Hong Kong, China
ORCID: https://orcid.org/0000-0002-7200-3695
Email: cejhyin@polyu.edu.hk

and
Wei-Qiang Feng
1: Assistant Professor, Department of Ocean Science and Engineering, Southern University of Science and Technology, Shenzhen, China
2: Southern Marine Science and Engineering Guangdong Laboratory (Guangzhou), Guangzhou, China.
ORCID: https://orcid.org/0000-0001-5480-9719
Email: fengwq@sustech.edu.cn

Manuscript submitted to *Engineering Geology* for possible publication

© 2023. This manuscript version is made available under the CC-BY-NC-ND 4.0 license https://creativecommons.org/licenses/by-nc-nd/4.0/.

Abstract: The thermal effects on geomaterials, especially on clayey soils are getting increasing concerns in many geotechnical applications. To study the effects of temperature on the stress-strain behaviour of Hong Kong marine deposits (HKMD), a series of temperature-controlled experiments were carried out. Oedometer and constant-rate-of-strain consolidation tests under temperatures from 10 °C to 60 °C were conducted on both intact and reconstituted HKMD considering different temperatures and stress paths. The effects of temperature history on the compression curves, thermally induced strain, and the characteristics of creep are revealed and discussed. The concept of virgin heating is proposed for interpreting the thermal plastic deformation. With increasing temperature, the creep coefficient is found to decrease while the creep strain rate increases. Consolidated undrained triaxial tests were performed on intact and reconstituted HKMD under different strain rates and temperature conditions. Under constant temperature, the undrained shear strength of HKMD is not significantly influenced by temperature. In triaxial tests subjected to step-changed temperature, the undrained heating causes a significant reduction of effective stress and rise of porewater pressure in HKMD. Finally, microscopic investigations with mercury intrusion porosimeter and scanning electron microscope are presented and discussed in this paper. It is found that the micropores of HKMD are evolutional with temperature.

Keywords: temperature, clayey soils, compression, shear behaviour, micro-structure, time-dependency

1 Introduction

Clayey soils are widely distributed in the sedimentary layers around the world and are related to a lot of geohazards and geotechnical problems such as slope instability, excessive settlement, embankment failure, *etc.*, which have been extensively studied in the past decades. In more recent years, the thermal effect on clayey soil behaviour has been another concern for various engineering practices, such as the thermo-boosted soil improvement (Abuel-Naga et al., 2006a; Chen et al., 2022), marine pipeline engineering (Scheiner et al., 2006; Shahrokhabadi et al., 2020; Thusyanthan et al., 2011), buffer of nuclear waste (Cui et al., 2009; Houston et al., 1985; Romero et al., 2005), energy piles (Brandl, 2006; Guo et al., 2020), tunnel fire (Chen et al., 2016), *etc*. Since the middle 20th century, researchers have experimentally investigated the temperature effects on the mechanical properties of different types of soft soils, the main findings from which can be summarized as follows.

Form the compression behaviour, the temperature-dependent yielding stress or thermally induced volume changes have been independently observed on different clayey soils. Researchers found that the yielding stress of soft soils decreases with temperature, while the compression index and recompression index were found to be less sensitive to temperature in most of studies (Abuel-Naga et al., 2006b; Campanella and Mitchell, 1968; Jarad, 2016; Li et al., 2018; Moritz, 1995; Paaswell, 1967; Tidfors and Sällfors, 1989). Nevertheless, some different results have been presented where the compression index was reduced with heating (Sultan et al., 2002; Tsutsumi and Tanaka, 2012). The thermally induced volume change under constant stress has been extensively investigated as well (Hueckel and Baldi, 1990; Towhata et al., 1993; Modaressi and Laloui, 1997; Burghignoli et al., 2000; Delage et al., 2000; Sultan et al., 2002; Abuel-Naga et al., 2007a; Coccia and McCartney, 2016a), and in most cases, clayey soils experienced cooling-

induced dilation and heating-induced contraction, the latter of which obviously decreases with the increasing over-consolidation ratio. However, systematic experimental and theoretical investigations to connect the temperature dependent yielding and thermal compression of clayey soils are scarcely reported. The effects of temperature history were also little investigated and limitedly understood.

Time-dependency is an important mechanical characteristic of soft clayey soils. Previous studies have found that under a constant stress, the strain rate is increased upon heating (Burghignoli et al., 2000; Cui et al., 2009; Fox and Edil, 1996). Some studies suggested that the secondary consolidation coefficient increases with temperature (Fox and Edil, 1996; Kaddouri et al., 2019), while others did not reveal a distinct trend (Jarad, 2016; Li et al., 2018), although some claims on the increasing trend were made. For the rate-dependent compression of soft soils, some researchers suggested that the rate-dependency of pre-consolidation pressure is similar under different temperatures (Boudali et al., 1994; Jarad, 2016; Marques et al., 2004), while others revealed non-isotach behaviour under a higher temperature (Tsutsumi and Tanaka, 2012). Given contradictory results were reported by different researchers, a systematic investigation and clarification on the rheological behaviour of clayey soils is demanded. The creep behaviour and its characterization under different temperatures should be clarified.

For the shear behaviour, researchers have conducted triaxial shearing tests under different temperature conditions on different kinds of clayey soils. Many concluded that the shear strength of clayey soils increases with consolidation temperature, while the critical state line is almost unaffected by temperature (Cekerevac and Laloui, 2004; Tanaka et al., 1997; Wang et al., 2020). Some studies however, reported an insignificant or reverse trend of shear strength with temperature (Burghignoli et al., 2000; Moritz, 1995). Besides, it was found that undrained heating in triaxial

tests can reduce the shear strength of soils (Hueckel and Pellegrini, 1992). However, parallel experiments for the different thermal effects under drained and undrained conditions on the shear behaviour with solid explanation are yet rarely presented.

The complicated thermo-mechanical behaviour of soft soils is closely related to the responses of the microstructures. Existing studies have attributed the thermal effects on the macro-behaviour to different mechanisms, including the changes of thickness of double layer water (Brochard et al., 2017; Towhata et al., 1993), inter-particle electrochemical forces (H. M. Abuel-Naga et al., 2007a), inter-particle macropores (Houhou et al., 2021), *etc.* To date, no consensus has been established on this issue.

In this study, a systematic experimental study scheme was carried out on a typical soft marine clayey soil. Different temperature-controlled laboratory tests, including oedometer tests, constant-rate-of-strain tests and triaxial tests were conducted to investigate the temperature effects on the compression and shear behaviour of soft soils with consideration of time dependency, temperature path and stress history. SEM tests and MIP tests were conducted to investigate the thermal effects on the micro-structure and pores of the clayey soil. The results from different tests are discussed in details and new concepts are proposed to form a better scientific understanding on the temperature and time dependent stress-strain behaviour of clayey soils.

2 Test materials, apparatus and procedures

2.1 Hong Kong marine deposits

The material used in the experiments was the Hong Kong marine deposits (HKMD), which is a typical soft marine clayey soil in Hong Kong (Yim, 1994). The particle size distribution is shown in Fig. 1 and the basic properties of HKMD used in this study are listed in Table 1.

Both intact and reconstituted HKMD was used in the test studies. The intact HKMD was provided by a construction site in Hong Kong, with an initial void ratio of around 1.6. The sample was retrieved and protected with commercially used thin-walled sampler, and therefore the integrity and structure of the soils are believed to be well preserved. To prepare the reconstituted samples, the same soil was totally remoulded and mixed with water to prepare a slurry. The HKMD slurry was poured into a steel cylinder and dead wight was applied on the soil for pre-consolidation. After that, test specimens were cut with dimensions of $\phi 62\text{mm} \times H 20\text{mm}$ for 1-D compression tests and $\phi 74\text{mm} \times H 152\text{mm}$ for triaxial tests.

2.2 Modified oedometer and triaxial cells with temperature control

A test apparatus was developed with a temperature control system for the oedometer and constant-rate-of-strain (CRS) tests, as shown in Fig. 2. The apparatus mainly consisted of a metal shell, a confining ring for holding the specimen, a porewater pressure transducer (PWPT) connected to the impermeable bottom of the soil, a linear variable differential transformer (LVDT) and a loading piston. It was a sealed system and back pressure was applied using a GDS pressure controller for fully saturation of the soil. For temperature control, an aluminium pipe was manufactured in a spiral shape and fixed inside the oedometer cell for fluid circulation. The spiral was connected to a temperature-controlled water bath with a circulation pump. The heat between the water bath and the oedometer cell is transferred through the water circulation in a constant rate of flow. Two temperature sensors were installed in the oedometer cell to monitor the stability of temperature control during the tests. For the oedometer tests, a leverage system was used for applying the vertical load. For CRS tests, the loading was applied by displacement control with a triaxial loading frame (VJ Tech, UK).

158 The temperature-controlled triaxial apparatus was developed based on a triaxial loading
159 frame (VJ Tech, UK) with both external and internal load cells, a PWPT, an LVDT, a data logging
160 system, a triaxial pressure cell and a set of water pressure controllers for back and cell pressure by
161 adding a self-developed temperature control system. Similar to the oedometer cell, an aluminium
162 pipe was manufactured in a spiral shape, fixed inside the triaxial cell and connected to a water bath
163 with a circulation pump. The setup of the whole system has been shown in Fig. 3.

164 To avoid disturbance to the soil specimen, temperature sensors were not installed inside
165 the soil during the tests. Calibration tests were carried out for the correlations among the
166 temperatures inside soil specimen, pressure cell and water bath. The calibration results can be
167 found in Fig. 4. Calibration tests on the thermal expansion and contraction of the system were
168 also carried out before formal experiments in the oedometer, CRS and triaxial test apparatus.
169 Changes of LVDT readings were collected during the heating and cooling cycles in absence of soil
170 specimen to calculate the thermally induced deformation of the system. For all the experiments,
171 the deformation of the specimen was corrected accordingly in analysing the strain data. For the
172 triaxial tests, the corrections for specimen area, membrane and other items were also included in
173 the data analysis (ASTM, 2011; Liu et al., 2020).

174

175 ***2.3 Test scheme***

176 The test scheme of temperature and vertical loading for the oedometer tests is shown in
177 Table 2. Three groups of temperature-controlled oedometer tests under 20 °C, 40 °C and 60 °C
178 (Oed-20, Oed-40, Oed-60) were carried out to investigate the 1-D consolidation and creep
179 behaviour of reconstituted HKMD under different constant temperatures. Two oedometer tests
180 with step-changed temperature condition (Oed-TP, TP means temperature path) were conducted

on both reconstituted and intact HKMD, for which heating-cooling cycle was applied under constant loadings.

Four groups of CRS tests were carried out on reconstituted HKMD under 10 °C, 20 °C, 40 °C and step-changed temperature, as shown in Table 3. Various loading rates and procedures for loading, unloading and reloading were involved in each CRS test.

Five consolidated undrained (CU) triaxial tests under constant temperature from 10 °C to 60 °C were carried out to investigate the thermal effects on the shear behaviour of HKMD, as shown in Table 4. In each test, step-changed shear strain rate was considered to reveal the rate effects (Feng et al., 2017b).

Five consolidated undrained triaxial tests under step-changed temperature condition were conducted on intact and reconstituted HKMD to investigate the effects of undrained heating on the shear behaviour of the soil specimens, as shown in Table 4. Different thermal conditions and over-consolidation ratios were considered for comparisons.

3 Temperature effects on the one-dimensional compression behaviour

3.1 Effects of constant temperatures

3.1.1 Normal compression and recompression index

Fig. 5 shows the 24 hours $e-\ln\sigma_z^{'}$ curves of HKMD under three different temperatures from the multi-stage loading oedometer tests. The normal compression index λ is calculated as the slope of the normal compression line (NCL) after yielding, which is also termed as "reference time line" (Yin and Graham 1994). The recompression index κ represents the elastic compression behaviour of soils and is fitted as the slope the unloading-reloading line (URL, also termed "instant

time line"), in which the visco-plastic strain is neglected. As indicated in Table 5, the values of λ and κ are not sensitive to temperature.

3.2.2 Temperature-dependent yielding stress

As shown in Fig. 5, the apparent pre-consolidation pressure σ'_{zp} at different temperatures can be calculated as the intersection between the fitted NCL and elastic instant time line in $e - \log\sigma'_z$ space, which also represents the yielding stress. The fitting results are listed in Table 5. It can be found that σ'_{zp} decreases with temperature from 20 to 60 °C, similar to the results reported in literatures for other clayey soils (Abuel-Naga et al., 2006b; Boudali et al., 1994; Campanella and Mitchell, 1968; Laloui and Cekerevac, 2003; Tidfors and Sällfors, 1989).

3.2 Effects of temperature changes

3.2.1 Strain-temperature relations

Figs. 6 and 7 show the typical results of compression and excess porewater pressure curves from the oedometer tests under step-changed temperature. Under constant loading, heating causes additional consolidation process for both intact and reconstituted HKMD specimens. Excess porewater pressure at the base of specimen exhibits an immediate rise due to heating and gradually dissipated with time. The process of cooling produces the opposite effects.

The changes of void ratio at 24 hours after temperature changes for the two HKMD specimens are plotted in Fig. 8. The thermally induced volumetric strain is highly dependent on the temperature history. Heating imposes irreversible compression to the NC soils, while cooling causes reversible and much smaller strains, which is similar to the results for other types of soils in the literature (Campanella and Mitchell, 1968; Cekerevac and Laloui, 2004; Coccia and

McCartney, 2016b). Furthermore, this study revealed the significant differences between virgin heating, cooling and re-heating. The virgin heating process could be regarded as a temperature-induced yielding mechanism, similar to the virgin compression (normal compression) in conventional soil mechanics, while the cooling and re-heating are similar to the elastic swelling and recompression process.

It is also found that increasing and decreasing the temperature for HKMD with an OCR of 2 (unloaded from 1200 kPa to 600 kPa) will impose much smaller volumetric strain compared with that for normally consolidated HKMD. Such results are similar to those mentioned in literatures (H. M. Abuel-Naga et al., 2007a; Laloui and Cekerevac, 2003; Modaressi and Laloui, 1997). In fact, the thermal strain with OCR=2 seems to be elastic, the slope of which is close to the cooling-induced strain under a normally consolidated state. The results suggest that within the yielding surface formed by historical maximal loading, the thermally induced strain is reversible.

The above observations indicate that there exists a temperature-stress hybrid yielding boundary formed by the historical maximal stress and temperature. Within this yielding boundary, the thermally induced strain is reversible, similar to the swelling and recompression process. The thermal elastic strain of HKMD is almost constant under different stress-strain states. If the new temperature goes beyond this boundary, irreversible strain will occur.

In addition, the slope of strain-temperature variation under virgin heating for normally consolidated reconstituted soils are found similar irrespective of different vertical stress. However, for intact HKMD, the slope gradually decreases with vertical stress, and is larger compared with reconstituted HKMD. It could be explained by the destructuration of the intact soil under heating, which contributes the magnification of plastic strain. With the increase of vertical loading, the structuration becomes smaller, and the soil behaviour is closer to the reconstituted HKMD.

3.2.2 Stress-strain curves with temperature history

Fig. 9 shows the 24 hours $e-\ln\sigma_z^{'}$ curves for the step-changed temperature oedometer with comparisons to the constant temperature oedometer tests. Good consistence can be found between the two types of oedometer tests. At the normal compression state, increasing the temperature from 20 °C, 40 °C to 60 °C will cause reduction of void ratio under the same effective stress. After cooling back to 20 °C, the volumetric changes are not recovered. However, with an increment of vertical loading under 20 °C, the stress-strain state evolves back to the original track of NCL. In contrast, when the soil is directly loaded to a new stress state under 60 °C, a parallel but lower NCL will be obtained. The normal compression lines obtained from the stress-strain points under 20 °C, 40 °C and 60 °C were close to those from constant temperature tests Oed-20, Oed-40 and Oed-60 (Oed-40 and Oed-60 were performed for the reconstituted HKMD only). Based on these findings, it can be inferred that there exists a unique NCL for each temperature, which is independent of the stress or temperature path. A virgin heating process on the normal consolidation state will break through the current yielding boundary, cause additional compression and generate a new NCL corresponding to the new temperature. In contrast, the cooling process is similar to the unloading process and will generate an over-consolidation state without changing the NCL.

Based on these discussions, the NCL of soils under different temperature can be expressed as:

$$\varepsilon_z = \varepsilon_{z0} + \frac{\kappa}{V}\ln\frac{\sigma_{zp0}^{'}}{\sigma_{z0}^{'}} + \frac{\lambda}{V}\ln\frac{\sigma_z^{'}}{\sigma_{zp0}^{'}} + \Delta\varepsilon_z^T \quad (1)$$

where $\left(\sigma_{z0}^{'},\varepsilon_{z0}\right)$ is the initial stress-strain state, $\sigma_{zp0}^{'}$ is the pre-consolidation pressure, ε_{zp0} is the strain under $\sigma_{zp0}^{'}$ on the normal compression line, $V=1+e_0$ is the initial specific volume, $\lambda=C_c\ln 10$ is the normal compression index, $\kappa=C_c\ln 10$ is the recompression index, $\Delta\varepsilon_z^T$ represents the strain caused by the virgin heating process. Substituting the following equations: $\varepsilon_z=\varepsilon_{z0}+\frac{\kappa}{V}\ln\frac{\sigma_{zp}^{'}}{\sigma_{z0}^{'}}+\frac{\lambda}{V}\ln\frac{\sigma_z^{'}}{\sigma_{zp}^{'}}$ into Eq. (1), the value of $\Delta\varepsilon_z^T$ can be expressed as:

$$\Delta\varepsilon_z^T=\frac{\kappa-\lambda}{V}\ln\frac{\sigma_{zp}^{'}}{\sigma_{zp0}^{'}} \tag{2}$$

With Eq. (2), the thermally strain and temperature dependent yielding stress can be correlated. The heating-induced plastic strain could be regarded as a result of shrinkage of current yielding boundary, which also leads to the reduction of yielding stress with increasing temperature.

3.3 Thermal effects on the time-dependent behaviour

3.3.1 Creep coefficient

For the constant temperature oedometers, the creep coefficient ψ was fitted as the slope of the linear $e-\ln t$ curve after primary consolidation at normal consolidation state (*i.e.*, 150, 300, 600 and 1200 kPa in this study). For the step-changed temperature tests, there exists a similar creep trend at after fully dissipation of excess porewater pressure in each $\varepsilon_z-\log t$ curve under either mechanical loading or virgin heating, as indicated in Fig. 6.

As shown in Fig. 10, although with some discrepancies, the creep coefficient ψ generally decreases with both temperature and vertical stress. However, the higher temperature, the less sensitivity of ψ to stress. The results are generally in agreement with some previous studies on natural and reconstituted clays (Feng et al., 2017a; Li et al., 2018; Yin, 1999). It can be attributed

to the movement of adsorbed water among the clay particles under the increase of temperature. The less residual adsorbed water, the smaller overall viscosity of the soil, the lower creep coefficient in the tests.

Meanwhile, good consistence is obtained between two types of oedometer tests, despite of some minor differences. This implies that a step-changed temperature oedometer test is enough to determine the temperature-dependent compressive behaviour instead of a series of constant-temperature oedometer tests, which can save time and cost for engineering and research purposes. For calculation of ψ at different temperatures, the elapsed time t should be started from the application of a new heating or loading stage. From Figs. 9 to Fig. 10, it is further proved that the virgin heating state of a normally consolidated clayey soil is equivalent to the normal compression state under the corresponding temperature.

3.3.2 Creep strain rates

The creep of soils can also be described through the rate of visco-plastic strain $\dot{\varepsilon}_z^{vp}$. From the oedometer tests, the value of $\dot{\varepsilon}_z^{vp}$ can be calculated using a secant approximation method:

$$\dot{\varepsilon}_{z,i}^{vp} = \left.\frac{\partial \varepsilon_z^{vp}}{\partial t}\right|_i \approx \left(\frac{\varepsilon_{z,i+1}^{vp} - \varepsilon_{z,i-1}^{vp}}{t_{i+1} - t_{i-1}}\right) \tag{3}$$

where t_i is the elapsed time at the moment, t_{i-1} and t_{i+1} are the time points before and after t_i, ε_z^{vp} is the elapsed vertical creep strain. With this method, the calculated values of $\dot{\varepsilon}_z^{vp}$ under different temperatures from the step-changed temperature oedometers under 300 kPa of vertical stress have been plotted in Fig. 11.

According to Fig. 11, the creep rate of HKMD decreases with elapsed vertical strain under a constant temperature. However, when temperature is increased, the creep rate has a sudden

increase, and then decreases again with elapsed strain after the balance of temperature, similar to the results presented in Chen and Yin (2023). The $\ln \dot{\varepsilon}_z^{vp} - \varepsilon_z$ curves under three temperatures are almost parallel to each other. According to the 1-D EVP model proposed by Yin and Graham (1994), the creep rate is expressed as:

$$\dot{\varepsilon}_z^{vp} = \frac{\psi}{Vt_0} \cdot \exp\left[-\frac{V}{\psi}\left(\varepsilon_z - \varepsilon_{zp0} \right) \right] \cdot \left(\frac{\sigma_z^{'}}{\sigma_{zp0}^{'}} \right)^{\frac{\lambda}{\psi}} \tag{4}$$

where $\sigma_{zp0}^{'}$ is the pre-consolidation pressure, ε_{zp0} is the strain under $\sigma_{zp0}^{'}$ on the normal compression line, $V = 1 + e_0$ is the initial specific volume, $\lambda = C_c \ln 10$ is the normal compression index, $\psi = C_\alpha \ln 10$ is the creep coefficient, t_0 is the reference time. From Equation (4), there is a linear relationship between $\ln \dot{\varepsilon}_z^{vp}$ and ε_z under a constant effective stress. The results from Fig. 11 are consistent with this model. However, under different temperatures, the $\ln \dot{\varepsilon}_z^{vp} - \varepsilon_z$ lines are shifted. To account for temperature-induced shifting of the $\ln \dot{\varepsilon}_z^{vp} - \varepsilon_z$ curves, Eq. (4) can be modified as:

$$\dot{\varepsilon}_z^{vp} = \frac{\psi}{Vt_0} \cdot \exp\left[-\frac{V}{\psi}\left(\varepsilon_z - \Delta\varepsilon_z^T - \varepsilon_{zp0} \right) \right] \cdot \left(\frac{\sigma_z^{'}}{\sigma_{zp0}^{'}} \right)^{\frac{\lambda}{\psi}} \tag{5}$$

where $\Delta\varepsilon_z^T$ is a temperature dependent strain accounting for the shifting of the $\ln \dot{\varepsilon}_z^{vp} - \varepsilon_z$ lines in Fig. 11. According to Eq. (5), the increased creep rate under heating is due to the positive $\Delta\varepsilon_z^T$, since ψ is not increasing according to the oedometer test results. According to Fig. 11 and Fig. 8, the value of $\Delta\varepsilon_z^T$ in Eq. (5) and Eq. (1) is quite close.

3.3.3 Isotach compression

Constant-rate-of-strain compression tests under different temperatures were conducted, as shown in Table 3. Fig. 12(a) shows the measured compression (ε_z - $\log \sigma_z^{'}$) curves of HKMD under constant temperatures (CRS-10, CRS-20 and CRS-40). According to the figure, the NCL under the same strain rate (*i.e.,* isotach) generally move downward with temperature from 10 °C, 20 °C to 40 °C, which is in accordance with the results from oedometer tests and the literatures (Boudali et al., 1994; Jarad, 2016; Marques et al., 2004). Besides, all the NCLs exhibit strain rate-dependency under all temperatures. The higher strain rate, the higher NCL. It is also found that the unloading-reloading line seems to be independent on the temperature, which is consistent with the constant recompression index from the oedometer tests.

Fig. 12(b) plots the compression curves of HKMD from a CRS test with step-changed temperatures from 10 °C., 20 °C., 40 °C to 60 °C. With the increase of temperature, the NCL under equal strain rate (*i.e*., isotach) is moved downward accordingly but still parallel to the original isotach under the subsequent loading. The higher temperature increment, the larger deviation from the original compression line. Therefore, the results from CRS tests further confirm the temperature-induced reduction of yielding stress and temperature-independency of normal compression index of HKMD.

4 Temperature effects on the triaxial shear behaviour

4.1 Temperature induced isotropic consolidation

Details of the triaxial tests are described in Table 4. The specimens for CU-10A, 10B, 20, 40 and 60 were consolidated under an isotropic stress of 300 kPa for 24 hours under 20 °C except CU-10A under 10 °C. The excess porewater pressure was fully dissipated within this time period. After that, the temperature condition was changed and sustained in drained condition for another

24 hours before the undrained compression tests. The thermally induced changes of void ratio Δe for different temperatures are shown in Fig. 13. The heating induced compression from 20 °C, 40 °C to 60 °C exhibited an increasing trend. The cooling induced volume changes from 20 °C to 10 °C can be nearly neglected. The trends are similar to the results in the last section under 1-D consolidation condition, as shown in Fig. 13.

4.2 Effects of constant temperature on shearing

4.2.1 Deviatoric stress-strain behaviour

Fig. 14(a) shows the deviatoric stress-strain ($q-\varepsilon_a$) curves of HKMD under different temperature conditions from the consolidated undrained shear texts. Several characteristics can be captured as follows.

First of all, the $q-\varepsilon_a$ curves of all tests exhibited sensitivity to rate of shear strain. In general, the higher strain rate, the higher deviatoric stress, which is similar to the results indicated in literatures (Fodil et al., 1997; Yin et al., 2002). However, such rate sensitivity of CU-40, CU-60 under higher temperature was smaller, which indicates that soils under higher temperature exhibits less viscous shearing behaviour.

Secondly, although the $q-\varepsilon_a$ curves of CU-10A, CU-20, CU-40 and CU-60 show limited distinction especially during the first loading stage, the values of q slightly increases with temperature at the later stages. It may be inferred that a higher temperature will increase the undrained shear stress after a certain range of deviatoric strain. However, such effect is insignificant, which is quite different from the results in some literature (Abuel-Naga et al., 2009; Cekerevac and Laloui, 2004; Wang et al., 2020, 2016), but similar to others (Burghignoli et al., 2000; Moritz, 1995). The improvement of shear strength might be attributed to the increasing

anisotropy under higher temperature as suggested by Abuel-Naga et al. (2009) and the densification of soil skeleton after heating, which is rather moderate for HKMD compared with the those in the literatures as revealed in the oedometer tests.

Besides, the shear stress of CU-10B is higher than CU-10A at the initial stage but converges to a similar level at the critical state. Similar trend has been reported on natural clays by Burghignoli et al. (2000), where the specimen after a thermal cycle exhibited an over-consolidated characteristic. The reason is that CU-10B was consolidated under 20 °C before cooling to 10 °C. Since the compression was irreversible during cooling, CU-10B became slightly over-consolidated compared to CU-10A and presented strain softening behaviour. Therefore, the shear strength was higher under the same confining stress.

4.2.2 Excess porewater pressure

Fig. 14(b) shows the measured excess porewater pressure u_e during the undrained shearing. For all tests, u_e ascended rapidly with the deviatoric strain. The differences of $u_e - \varepsilon_a$ curves for different temperature conditions were not significant.

4.2.3 Effective stress path

The effective stress ($q - p'$) paths of the CU tests are plotted in Fig. 14(c). The final stress state of different tests almost falls on a similar critical state line, although, the $q - p'$ points were rapidly changed with changes of strain rate. Under different temperatures, no significant difference was exhibited, except for CU-10B, the stress path of which showed a steeper trend and approached the critical state under a higher deviatoric stress.

Fig. 14(a) also shows that the slope of critical state line M_c of HKMD is not sensitive to temperature. Therefore, one may deduce that temperature does not produce significant changes on M_c of HKMD, as most of clayey soils in previous studies (H. M. Abuel-Naga et al., 2007c; Cekerevac and Laloui, 2004; Wang et al., 2020). It may be inferred that the friction angle, controlled by the mechanical forces between the solid particles, is not sensitive to the temperature and thermally induced visco-plastic strain.

4.3 Effects of temperature changes on undrained shearing

For the step-changed temperature CU tests, undrained heating was conducted during the undrained shearing process, which was different from the drained heating or cooling in tests CU-10A to CU-60.

4.3.1 Deviatoric stress-strain behaviour

Fig. 15(a) and Fig. 16(a) show the $q-\varepsilon_a$ curves of the intact and reconstituted HKMD samples under step-changed strain rates and temperatures. All of them exhibit sensitivity to strain rate. The larger strain rate, the higher deviatoric stress, similar to previous test studies on HKMD (Yin et al., 2002). The strain rate effect of deviatoric stress-strain exists during the whole shearing process, even near the critical state.

According to the figures, the step-changed temperature also has significant effects on the undrained shear behaviour. For CU-I2 and CU-R3 without change of temperature, the relaxation stage imposes a reduction of deviatoric stress, but the $q-\varepsilon_a$ goes back to the original track under the subsequent loading. For CU-I1, CU-R1 and CU-R2 however, after the temperature is increased by 20 °C, the deviatoric stress is largely reduced. With the subsequent loading, the $q-\varepsilon_a$ curve is

shifted downward rather than recover to the original track. The higher temperature, the lower position of $q-\varepsilon_a$ curve.

Comparing these results with Fig. 14(a), it can be found that the undrained heating and drained heating impose different effects on the shear behaviour of soils. As revealed in the consolidation tests, heating produces visco-plastic straining, which is controlled by the hybrid yielding boundary. The similar visco-plastic strain should occur in the triaxial condition. For undrained heating, the total mass of the specimen is unchanged and total volumetric strain is restricted. The visco-plastic straining will then force the elastic volume strain to decrease, and effective confining stress is immediately reduced, according to Hook's law. Such process will soften the soil and reduce the shear strength. This explanation can well answer the test results reported by Hueckel and Pellegrini (1992). Although CU-R2 has an over-consolidation ratio of 2, it has reached the yielding surface before heating, so the heating induced visco-plastic strain is similar to the normally consolidated one. The temperature-stress hybrid yielding boundary observed from 1-D could be extended to the hybrid yielding surfaces triaxial conditions.

For drained heating, excess porewater pressure is dissipated before shearing and the initial effective stress is not affected by different temperatures. If the heating induced compression causes hardening of the soil, the shear strength will be increased, as indicated in the literature (Abuel-Naga et al., 2009; Wang et al., 2020). From this study, it is clear that the hydraulic boundary condition plays an important role in the thermal effects on the shear strength of clayey soils, due to the visco-plastic strain produced during heating.

4.3.2 Excess porewater pressure

The excess porewater pressure plotted in Fig. 15(b) and Fig. 16(b) is remarkedly influenced by undrained heating. When the soil was subject to heating, excess porewater pressure rises and did not recover to the previous track under subsequent shearing. For CU-I2 and CU-R3 without heating, the excess porewater pressure slightly decreases during relaxation, but increases to the original track after reloading. This again verifies that undrained heating imposed unrecoverable changes of the soil skeleton and reduces the resistance of the soil against external loading.

4.3.3 Effective stress path

Fig. 15(c) and Fig. 16(c) show the $q - p'$ curves of the intact and reconstituted HKMD specimens. The effective stress path is notably influenced by the changes of strain rate and temperature. In all the tests, increasing the strain rate is accompanied with an expansion of the stress locus in $q - p'$ space, while either decreasing the strain rate or increasing the temperature induces a contraction of stress locus. Both mean effective stress and deviatoric stress are reduced, indicating that both volumetric and deviatoric visco-plastic strains are produced by undrained heating under triaxial condition.

However, the final stress state points under different strain rate and temperatures always fall onto the same critical state line. It can be concluded that changes of strain rate and temperature during the undrained shearing will change the effective stress level, but friction angle is not changed.

5 Effects of temperature on micro-structure

5.1 Particle arrangement and soil fabric

Scanning electron microscope (SEM) was used to investigate the microstructure of three specimens after oedometer tests: Oed-20, Oed-40 and Oed-60. After the final loading stage, the soil was completely unloaded, taken out from the confining ring, and cut carefully into beam shape. The water in the soil specimen was removed using a freeze-drying technique, which was aimed at minimizing the changes of microstructures during the air-drying process (Zhao, 2017). After the freeze-drying, the beam specimen was broken off from the middle across the section for observation. The scanning tests were conducted with a TESCAN VEGA3 system. Fig. 17 shows the scanning photos of HKMD specimens Oed-20, Oed-40, Oed-60 after oedometer tests under of 10,000 x magnification. The clay particles in all specimens exhibit an aggregated mode (Mitchell and Soga, 2005), with inter-aggregate and intra-aggregate pores. There is no sign that temperature could induce visible changes to the particle arrangement or other physicochemical properties of clayey soils.

SEM photos are commonly used to quantitatively evaluate the fabric of the soils by image processing and rose diagrams (Gao et al., 2020; Hicher et al., 2000; Zhao, 2017). In this study, five photos (5,000 x magnification) at different random positions for each sample are imported into the software ImageJ for analysis. The photos are processed with the unsharp mask filter and binarization, to obtain binary images of isolated pores between soil particles. The area and orientation of each pore is calculated by the software. As shown in Fig.17, the results of pore identification are generally accurate. Rose diagrams are plotted to show the pore area distribution in different orientations for three HKMD specimens. Most pore area is horizontally oriented (0 and 180 °), indicating the anisotropy fabric of HKMD under 1-D compression. Although one might observe that the horizontally oriented pores gain a slight growth from 20 to 60 °C, the differences

between three temperatures are not significant enough. Therefore, the fabric and anisotropy of HKMD is not significantly changed by temperature.

The abovementioned results from both qualitative and quantitative analysis may explain the micro mechanical behaviour of HKMD in the previous sections. The insignificant change of inter-particle arrangement characteristic should be the origin of some temperature-independent macro-properties, including the compression indices λ and κ, friction angle and critical state line, *etc*. Besides, the temperature effects on particle orientation and anisotropy are not visually obvious, while could explain the findings in the triaxial tests that anisotropy and shear strength were not insignificantly affected by the temperature.

5.2 Pore size distribution

To characterize the micropores in the HKMD specimen subjected to different temperatures, mercury intrusion porosimetry (MIP) tests were conducted on the freeze-dried specimen with a porosimeter (Micromeritics Instrument Corporation, USA). Four specimens were investigated, including three oedometer specimens with maximal loading of 1200 kPa under 20, 40, 60 °C, and one CRS specimen subjected to a maximal vertical effective stress of 837 kPa under 60 °C. Fig. 18 shows their pore size distribution curves. The differential intrusion is calculated by $\frac{\Delta V_{Hg}}{m_{soil}\Delta d_{pore}}$, representing the density function of pore volume for unit mass of dry soil.

According to the Fig. 18, the pore size of HKMD roughly follows a double-peaks distribution, and the boundary between two peaks is around 0.1 μm. The two peaks could be categorized into intra-aggregates and inter-aggregates pores respectively, as indicated in the literature (Chow et al., 2019; Hattab et al., 2013; Houhou et al., 2021; Tarantino and De Col, 2008; Yin et al., 2011).

512 For specimens Oed-20, Oed-40, and Oed-60, the higher temperature, the smaller volume
513 of the larger-pores peak. There is also a tendency of left-shift with increasing temperature,
514 indicating larger pores converted to smaller ones. Such behaviour could be the origin of decreasing
515 void ratio with temperature in the 1-D compression tests. For specimen CRS-TP, the historically
516 highest temperature is 60 °C, but the maximum loading is just 837 kPa, smaller than 1200 kPa of
517 Oed-60. The clear gap between CRS-TP and Oed-60 in Fig. 18 indicates that increasing stress also
518 contributes to contraction and left-shift of the larger-pores peak. Therefore, the mechanisms of
519 temperature and stress effects share some similarity. Both heating and loading will predominantly
520 reduce the volume of the larger pores, inducing plastic compressive strains in the soils, as discussed
521 in the previous sections.
522
523 **6 Conclusions**
524 A series of oedometer, constant-rate-of-strain consolidation and triaxial tests were
525 conducted for reconstituted and intact HKMD under different temperature conditions. The effects
526 of temperature on the volume compression, creep and shear behaviour are discussed based on the
527 experimental results. MIP and SEM tests were performed on clay samples after oedometer tests to
528 revel the influence of temperature on the microstructure of the soil. Several important findings and
529 conclusions can be drawn as follows:
530 (a) The pre-consolidation pressure of reconstituted HKMD decreases with temperature, while the
531 compression index λ and recompression index κ are almost unchanged under different
532 temperatures. Further, such effects are not influenced on the temperature history of the soils.
533 (b) The virgin heating on the normally consolidated HKMD will produce visco-plastic volumetric
534 strain, while the cooling process mainly causes elastic strain with similar magnitude to the

thermally induced strain of heavily over-consolidated HKMD. The slope of elastic $e-\ln T$ curves is almost a constant at different soil states. The slope of $e-\ln T$ under virgin heating at normal consolidation state is also similar under different vertical loadings, but larger for intact HKMD compared with reconstituted HKMD.

(c) For the tested HKMD, creep strain rate is increased instantly upon the increase of temperature. The creep coefficient ψ, fitted from the creep strain-time curves under a constant temperature and loading, is found to decrease with temperature.

(d) In the constant temperature CU tests, the undrained shear strength of HKMD may slightly increase with temperature, but not significantly. The drained heating-cooling process has similar effects to the over-consolidation on the shear behaviour of the soils. The critical state line and friction angle of HKMD is not sensitive to the temperature condition, as appearing in the all the CU tests.

(e) Undrained heating can cause reduction of effective stress and shear strength, rise of excess porewater pressure and pass-over on the critical state line, which could be attributed to the heating induced visco-plastic strain in the triaxial condition.

(f) According to the SEM results, the orientations of micropores are relatively stable under different temperatures, which could explain the temperature-insensitive compression indices, friction angle, and shear strength of HKMD. The MIP test results indicate that increasing the temperature cause contraction of the larger pores, similar to the effects of stress increment.

Acknowledgement

The work in this paper is supported by a Research Impact Fund (RIF) project (R5037-18), a Theme-based Research Scheme Fund (TRS) project (T22-502/18-R), and three General Research

Fund (GRF) projects (PolyU 152179/18E; PolyU 152130/19E; PolyU 152100/20E) from Research Grants Council (RGC) of Hong Kong Special Administrative Region Government of China. The authors also acknowledge the financial supports from a grant (CD82) from Research Institute for Land and Space, grants (ZDBS, BD8U) from The Hong Kong Polytechnic University, Shenzhen Science and Technology Innovation Commission (JCYJ20210324105210028), the Key Special Project for Introduced Talents Team of Southern Marine Science and Engineering Guangdong Laboratory (Guangzhou) (GML2019ZD0210) and a grant from Southern Marine Science and Engineering Guangdong Laboratory (Guangzhou) (K19313901).

References

Abuel-Naga, H. M., Bergado, D.T., Bouazza, A., 2007a. Thermally induced volume change and excess pore water pressure of soft Bangkok clay. Eng. Geol. 89, 144–154. https://doi.org/10.1016/j.enggeo.2006.10.002

Abuel-Naga, H.M., Bergado, D.T., Bouazza, A., Pender, M., 2009. Thermomechanical model for saturated clays. Géotechnique 59, 273–278. https://doi.org/10.1680/geot.2009.59.3.273

Abuel-Naga, H. M., Bergado, D.T., Bouazza, A., Ramana, G. V., 2007b. Volume change behaviour of saturated clays under drained heating conditions: Experimental results and constitutive modeling. Can. Geotech. J. 44, 942–956. https://doi.org/10.1139/T07-031

Abuel-Naga, H.M., Bergado, D.T., Chaiprakaikeow, S., 2006a. Innovative thermal technique for enhancing the performance of prefabricated vertical drain during the preloading process. Geotext. Geomembranes 24, 359–370. https://doi.org/10.1016/j.geotexmem.2006.04.003

Abuel-Naga, H. M., Bergado, D.T., Lim, B.F., 2007c. Effect of temperature on shear strength and yielding behavior of soft Bangkok clay. Soils Found. 47, 423–426. https://doi.org/10.3208/sandf.47.423

Abuel-Naga, H.M., Bergado, D.T., Ramana, G. V., Grino, L., Rujivipat, P., Thet, Y., 2006b. Experimental evaluation of engineering behavior of soft Bangkok clay under elevated temperature. J. Geotech. Geoenvironmental Eng. 132, 902–910. https://doi.org/10.1061/(asce)1090-0241(2006)132:7(902)

ASTM, 2011. D4767 − 11. Standard test method for consolidated undrained triaxial compression test for cohesive soils, ASTM International, West Conshohocken, PA, American Society for Testing and Materials.

Boudali, M., Leroueil, S., Murthy Srinivasa, B.R., 1994. Viscous behaviour of natural clays, in:

International Conference on Soil Mechanics and Foundation Engineering. pp. 411–416.

Brandl, H., 2006. Energy foundations and other thermo-active ground structures. Géotechnique 56, 81–122. https://doi.org/10.1680/geot.2006.56.2.81

Brochard, L., Honório, T., Vandamme, M., Bornert, M., Peigney, M., 2017. Nanoscale origin of the thermo-mechanical behavior of clays. Acta Geotech. 12, 1261–1279. https://doi.org/10.1007/s11440-017-0596-3

Burghignoli, A., Desideri, A., Miliziano, S., 2000. A laboratory study on the thermomechanical behaviour of clayey soils. Can. Geotech. J. 37, 764–780. https://doi.org/10.1139/t00-010

Campanella, R.G., Mitchell, J.K., 1968. Influence of temperature variations on soil behavior. J. Soil Mech. Found. Div. 94, 709–734. https://doi.org/10.1126/science.85.2195.95.b

Cekerevac, C., Laloui, L., 2004. Experimental study of thermal effects on the mechanical behaviour of a clay. Int. J. Numer. Anal. Methods Geomech. 28, 209–228. https://doi.org/10.1002/nag.332

Chen, Z.-J., Yin, J.-H., 2023. A new one-dimensional thermal elastic visco-plastic model for the thermal creep of saturated clayey soils. J. Geotech. Geoenvironmental Eng. https://doi.org/10.1061/JGGEFK/GTENG-10195

Chen, Z., Zhu, H., Yan, Z., Zhao, L., Shen, Y., Misra, A., 2016. Experimental study on physical properties of soft soil after high temperature exposure. Eng. Geol. 204, 14–22. https://doi.org/10.1016/j.enggeo.2016.01.014

Chen, Z.J., Feng, W.Q., Li, A., Al-Zaoari, K.Y.M., Yin, J.H., 2022. Experimental and molecular dynamics studies on the consolidation of Hong Kong marine deposits under heating and vacuum preloading. Acta Geotech. https://doi.org/10.1007/s11440-022-01735-x

Chow, J.K., Li, Z., Wang, Y.H., 2019. An experimental microstructural characterization of high-

quality, load-preserved fabric 1-D consolidated kaolinite samples. E3S Web Conf. 92, 1–5. https://doi.org/10.1051/e3sconf/20199201006

Coccia, C.J.R., McCartney, J.S., 2016a. Thermal volume change of poorly draining soils I: Critical assessment of volume change mechanisms. Comput. Geotech. 80, 26–40. https://doi.org/10.1016/j.compgeo.2016.06.009

Coccia, C.J.R., McCartney, J.S., 2016b. Thermal volume change of poorly draining soils II: Model development and experimental validation. Comput. Geotech. 80, 16–25. https://doi.org/10.1016/j.compgeo.2016.06.010

Cui, Y.J., Le, T.T., Tang, A.M., Delage, P., Li, X.L., 2009. Investigating the time-dependent behaviour of Boom clay under thermomechanical loading. Géotechnique 59, 319–329. https://doi.org/10.1680/geot.2009.59.4.319

Delage, P., Sultan, N., Cui, Y.J., 2000. On the thermal consolidation of Boom clay. Can. Geotech. J. 37, 343–354. https://doi.org/10.1139/t99-105

Feng, W.-Q., Lalit, B., Yin, Z.-Y., Yin, J.-H., 2017a. Long-term Non-linear creep and swelling behavior of Hong Kong marine deposits in oedometer condition. Comput. Geotech. 84, 1–15. https://doi.org/10.1016/j.compgeo.2016.11.009

Feng, W.-Q., Yin, J.-H., Tao, X.-M., Tong, F., Chen, W.-B., 2017b. Time and Strain-Rate Effects on Viscous Stress–Strain Behavior of Plasticine Material. Int. J. Geomech. 17, 04016115. https://doi.org/10.1061/(asce)gm.1943-5622.0000806

Fodil, A., Aloulou, W., Hicher, P.Y., 1997. Viscoplastic behaviour of soft clay. Géotechnique 47, 581–591. https://doi.org/10.1680/geot.1997.47.3.581

Fox, P.J., Edil, T.B., 1996. Effects of stress and temperature on secondary compression of peat. Can. Geotech. J. 33, 405–415.

636 Gao, Q.F., Hattab, M., Jrad, M., Fleureau, J.M., Hicher, P.Y., 2020. Microstructural organization
637 of remoulded clays in relation with dilatancy/contractancy phenomena. Acta Geotech. 15,
638 223–243. https://doi.org/10.1007/s11440-019-00876-w
639 Guo, Y., Zhang, G., Liu, S., 2020. Temperature effects on the in-situ mechanical response of
640 clayey soils around an energy pile evaluated by CPTU. Eng. Geol. 276, 105712.
641 https://doi.org/10.1016/j.enggeo.2020.105712
642 Hattab, M., Hammad, T., Fleureau, J.M., Hicher, P.Y., Mesri, G., 2013. Behaviour of a sensitive
643 marine sediment: Microstructural investigation. Geotechnique 63, 71–84.
644 https://doi.org/10.1680/geot.13.D.02
645 Hicher, P.Y., Wahyudi, H., Tessier, D., 2000. Microstructural analysis of inherent and induced
646 anisotropy in clay. Mech. Cohesive-Frictional Mater. 5, 341–371.
647 https://doi.org/10.1002/1099-1484(200007)5:5<341::AID-CFM99>3.0.CO;2-C
648 Houhou, R., Sutman, M., Sadek, S., Laloui, L., 2021. Microstructure observations in compacted
649 clays subjected to thermal loading. Eng. Geol. 287, 105928.
650 https://doi.org/10.1016/j.enggeo.2020.105928
651 Houston, S.L., Houston, W.N., Williams, N.D., 1985. Thermo-mechanical behavior of seafloor
652 sediments. J. Geotech. Eng. 111, 1249–1263. https://doi.org/10.1061/(ASCE)0733-
653 9410(1985)111:11(1249)
654 Hueckel, T., Baldi, G., 1990. Thermoplasticity of saturated clays: experimental constitutive
655 study. J. Geotech. Geoenvironmental Eng. ASCE 116, 1778–1796.
656 Hueckel, T., Pellegrini, R., 1992. Effective stress and water pressure in saturated clays during
657 heating-cooling cycles. Can. Geotech. J. 29, 1095–1102. https://doi.org/10.1139/t92-126
658 Jarad, N., 2016. Temperature impact on the consolidation and creep behaviour of compacted

clayey soils. Université de Lorraine.

Kaddouri, Z., Cuisinier, O., Masrouri, F., 2019. Influence of effective stress and temperature on the creep behavior of a saturated compacted clayey soil. Geomech. Energy Environ. 17, 106–114. https://doi.org/10.1016/j.gete.2018.09.002

Laloui, L., Cekerevac, C., 2003. Thermo-plasticity of clays: An isotropic yield mechanism. Comput. Geotech. 30, 649–660. https://doi.org/10.1016/j.compgeo.2003.09.001

Li, Y., Dijkstra, J., Karstunen, M., 2018. Thermomechanical creep in sensitive clays. J. Geotech. Geoenvironmental Eng. 144, 04018085. https://doi.org/10.1061/(asce)gt.1943-5606.0001965

Liu, K., Yin, J.H., Chen, W.B., Feng, W.Q., Zhou, C., 2020. The stress–strain behaviour and critical state parameters of an unsaturated granular fill material under different suctions. Acta Geotech. 15, 3383–3398. https://doi.org/10.1007/s11440-020-00973-1

Marques, M.E.S., Leroueil, S., de Almeida, M. de S.S., 2004. Viscous behaviour of St-Roch-de-l'Achigan clay, Quebec. Can. Geotech. J. 41, 25–38. https://doi.org/10.1139/t03-068

Mitchell, J.K., Soga, K., 2005. Fundamentals of soil behavior, 3rd ed. Wiley, New York.

Modaressi, H., Laloui, L., 1997. A thermo-viscoplastic constitutive model for clays. Int. J. Numer. Anal. Methods Geomech. 21, 709–734. https://doi.org/10.1002/(sici)1096-9853(199705)21:5<313::aid-nag872>3.0.co;2-5

Moritz, L., 1995. Geotechnical Properties of Clay at Elevated Temperatures. Linköping, Sweden. 69p.

Neaupane, K.M., Nanakorn, P., Sirayapivat, O., Kanborirak, S., 2005. Effects of temperature on 1-D consolidation characteristics of clayey soil, in: Proceedings of the 16th International Conference on Soil Mechanics and Geotechnical Engineering: Geotechnology in Harmony

with the Global Environment. pp. 417–420. https://doi.org/10.3233/978-1-61499-656-9-417

Paaswell, R.E., 1967. The effect of temperature on the consolidation of soils. J. Soil Mech. Found. Div. 93, 9–22.

Romero, E., Villar, M. V., Lloret, A., 2005. Thermo-hydro-mechanical behaviour of two heavily overconsolidated clays. Eng. Geol. 81, 255–268. https://doi.org/10.1016/j.enggeo.2005.06.011

Scheiner, S., Pichler, B., Hellmich, C., Eberhardsteiner, J., 2006. Loading of soil-covered oil and gas pipelines due to adverse soil settlements - Protection against thermal dilatation-induced wear, involving geosynthetics. Comput. Geotech. 33, 371–380. https://doi.org/10.1016/j.compgeo.2006.08.003

Shahrokhabadi, S., Cao, T.D., Vahedifard, F., 2020. Thermal effects on hydromechanical response of seabed-supporting hydrocarbon pipelines. Int. J. Geomech. 20, 04019143. https://doi.org/10.1061/(asce)gm.1943-5622.0001534

Sultan, N., Delage, P., Cui, Y.J., 2002. Temperature effects on the volume change behaviour of Boom clay. Eng. Geol. 64, 135–145. https://doi.org/10.1016/S0013-7952(01)00143-0

Tanaka, N., Graham, J., Crilly, T., 1997. Stress-strain behaviour of reconstituted illitic clay at different temperatures. Eng. Geol. 47, 339–350. https://doi.org/10.1016/s0013-7952(96)00113-5

Tarantino, A., De Col, E., 2008. Compaction behaviour of clay. Geotechnique 58, 199–213. https://doi.org/10.1680/geot.2008.58.3.199

Thusyanthan, N.I., Cleverly, W., Haigh, S.K., Ratnam, S., 2011. Thermal imaging , thermal conductivity of soil and heat loss from buried pipelines, in: The Offshore Pipeline Technology Conference. pp. 1–17.

Tidfors, M., Sällfors, G., 1989. Temperature effect on preconsolidation pressure. Geotech. Test. J. 12, 93–97.

Towhata, I., Kuntiwattanaku, P., Seko, I., Ohishi, K., 1993. Volume change of clays induced by heating as observed in consolidation tests. Soils Found. 33, 170–183. https://doi.org/10.3208/sandf1972.33.4_170

Tsutsumi, A., Tanaka, H., 2012. Combined effects of strain rate and temperature on consolidation behavior of clayey soils. Soils Found. 52, 207–215. https://doi.org/10.1016/j.sandf.2012.02.001

Wang, K., Wang, L., Hong, Y., 2020. Modelling thermo-elastic–viscoplastic behaviour of marine clay. Acta Geotech. 15, 2415–2431. https://doi.org/10.1007/s11440-020-00917-9

Wang, L.Z., Wang, K.J., Hong, Y., 2016. Modeling temperature-dependent behavior of soft clay. J. Eng. Mech. 142, 04016054. https://doi.org/10.1061/(asce)em.1943-7889.0001108

Yim, W.W.S., 1994. Offshore Quaternary sediments and their engineering significance in Hong Kong. Eng. Geol. 37, 31–50. https://doi.org/10.1016/0013-7952(94)90080-9

Yin, J.-H., 1999. Non-linear creep of soils in oedometer tests. Géotechnique 49, 699–707. https://doi.org/10.1680/geot.1999.49.5.699

Yin, J.-H., Zhu, J.-G., Graham, J., 2002. A new elastic viscoplastic model for time-dependent behaviour of normally and overconsolidated clays: theory and verification. Can. Geotech. J. 39, 157–173. https://doi.org/10.1139/t01-074

Yin, Z.-Y., Hattab, M., Hicher, P.-Y., 2011. Multiscale modeling of a sensitive marine clay. Int. J. Numer. Anal. Methods Geomech. 35, 1682–1702. https://doi.org/10.1002/nag

Zhao, D., 2017. Study on the creep behavior of clay under complex triaxial loading in relation to the microstructure. University of Lorraine.

728

ccList of Figure Captions

List of Tables

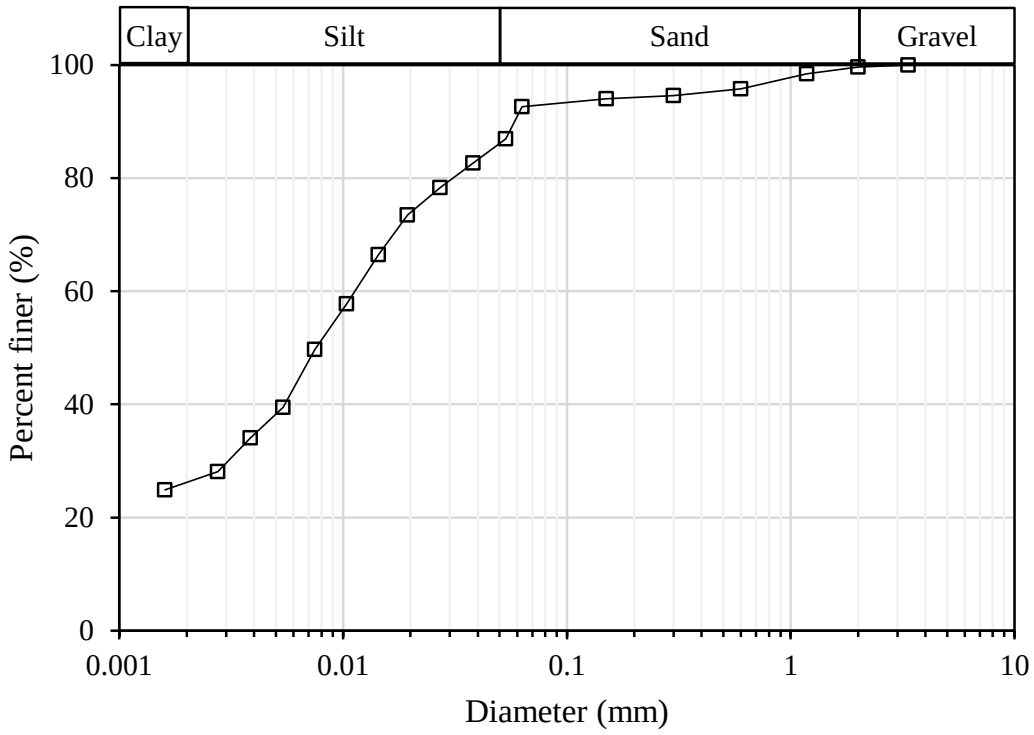

Fig. 1 Particle size distribution of the tested HKMD

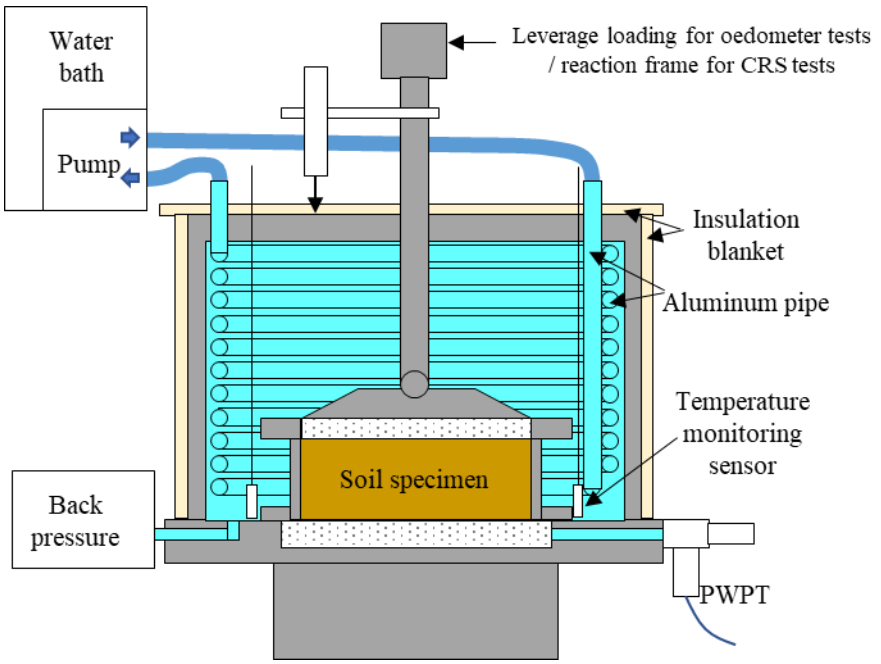

Fig. 2 Set-up of the temperature-controlled oedometer and CRS apparatus

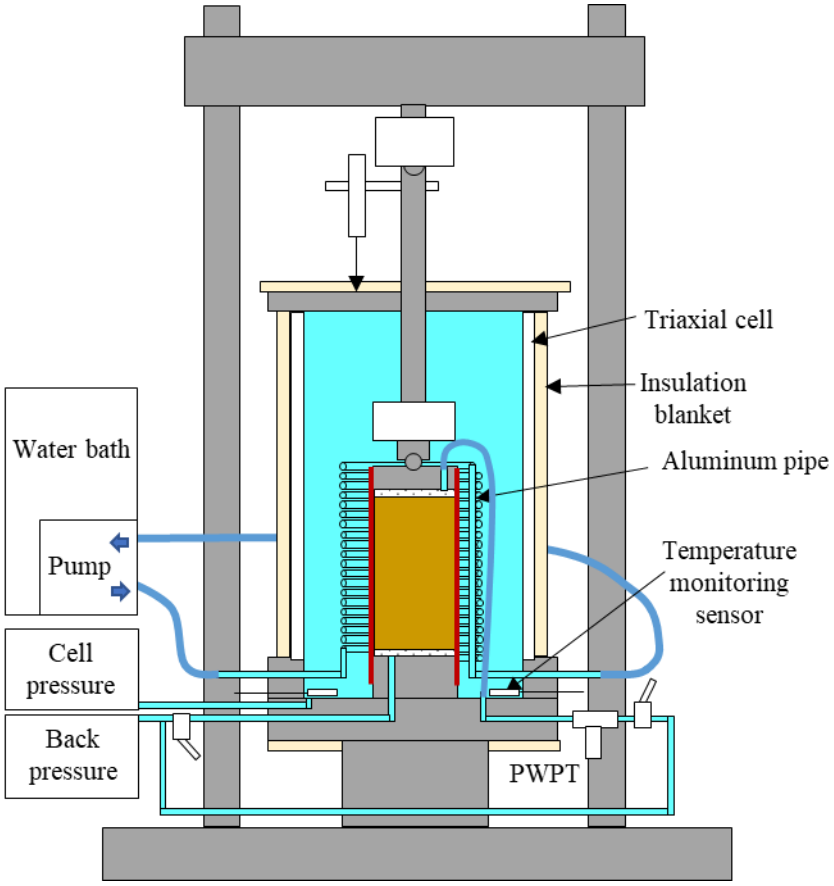

Fig. 3 Set-up of the temperature-controlled triaxial test system

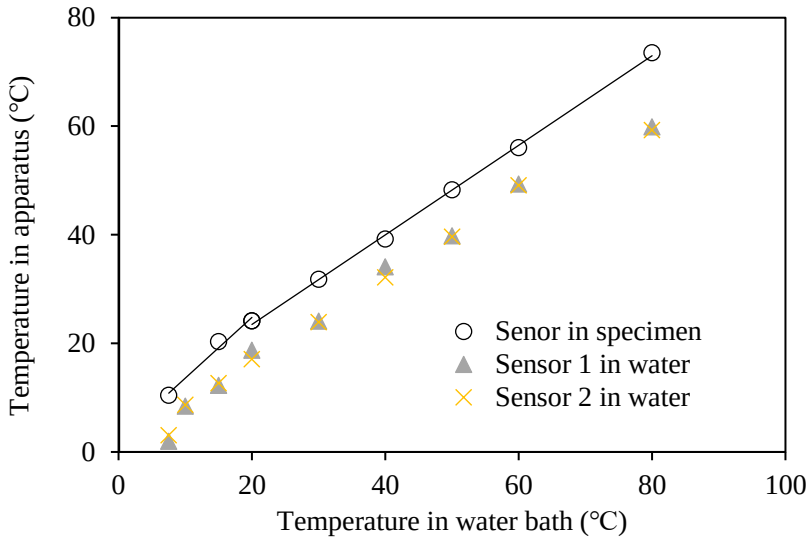

(a)

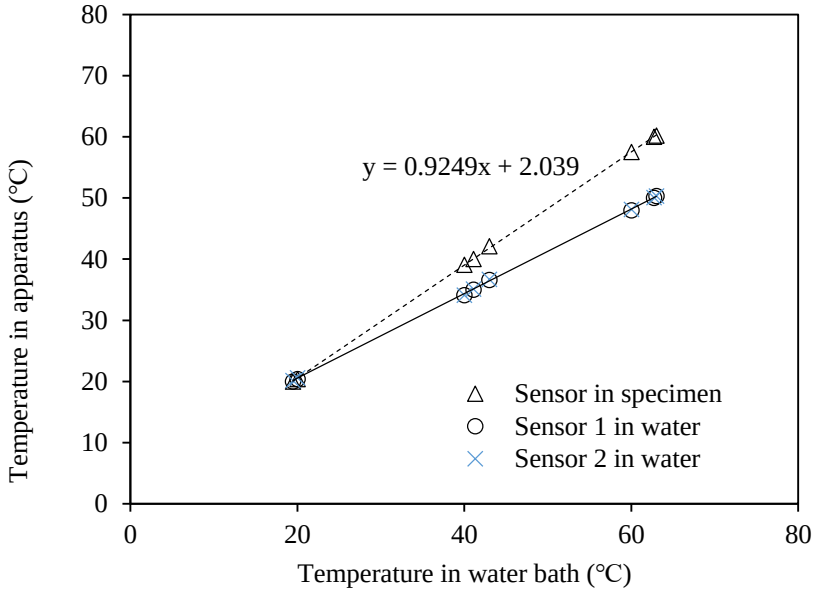

(b)

Fig. 4 Relations of temperature in the water bath, cell water and soil specimen in the test apparatus: (a) oedometer cell and (b) triaxial cell

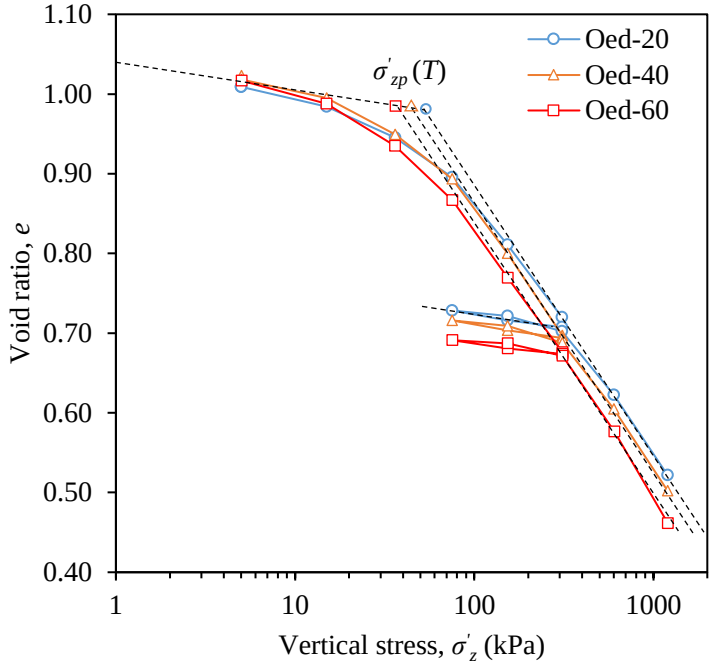

Fig. 5 1-D compression curves of reconstituted HKMD under different constant temperatures

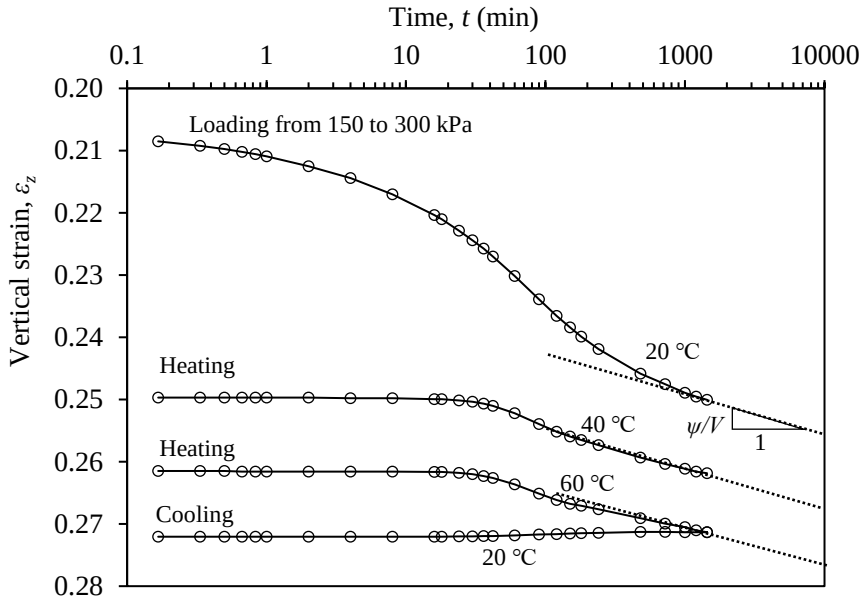

Fig. 6 Typical consolidation curves of reconstituted HKMD under step-loading, heating, and cooling

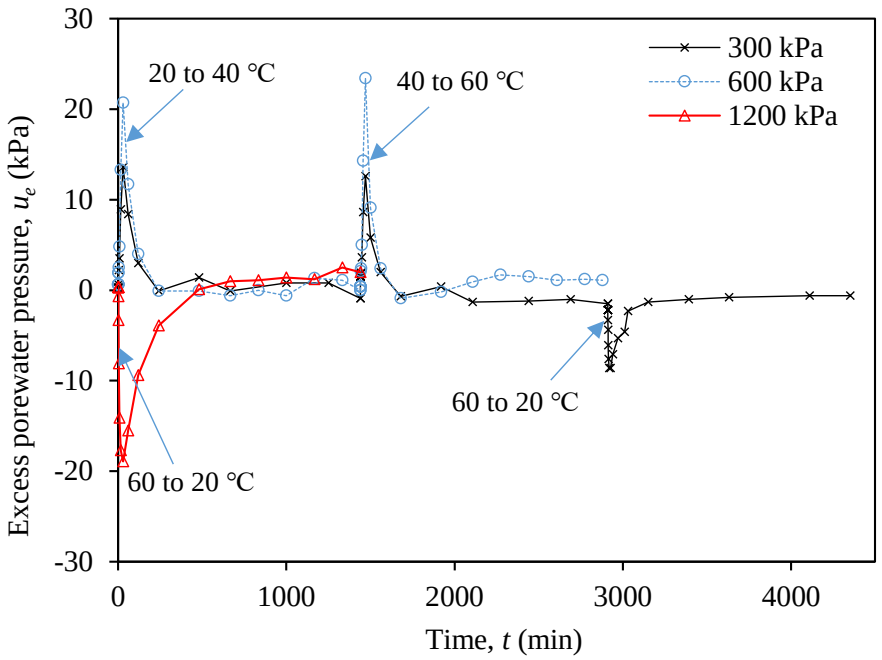

Fig. 7 Typical excess porewater pressure response under heating and cooling

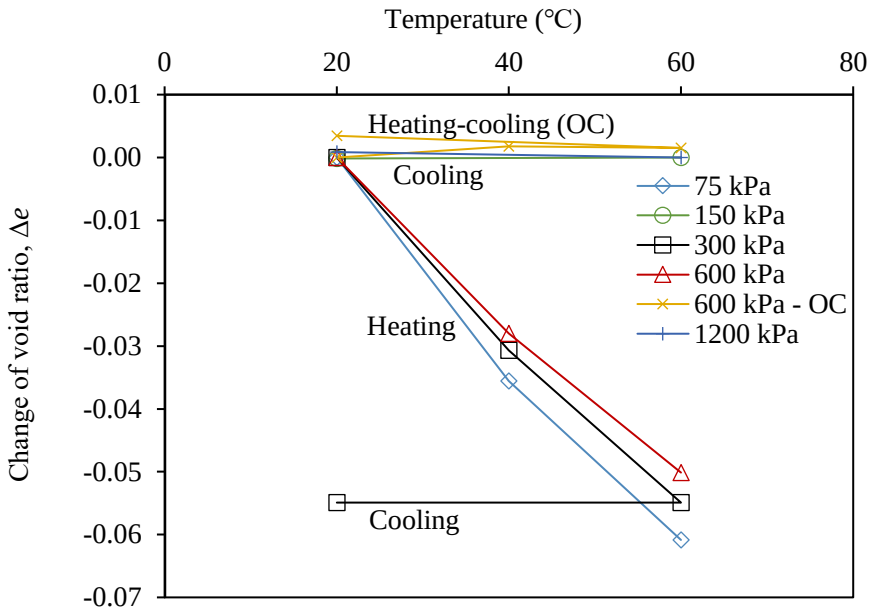

(a)

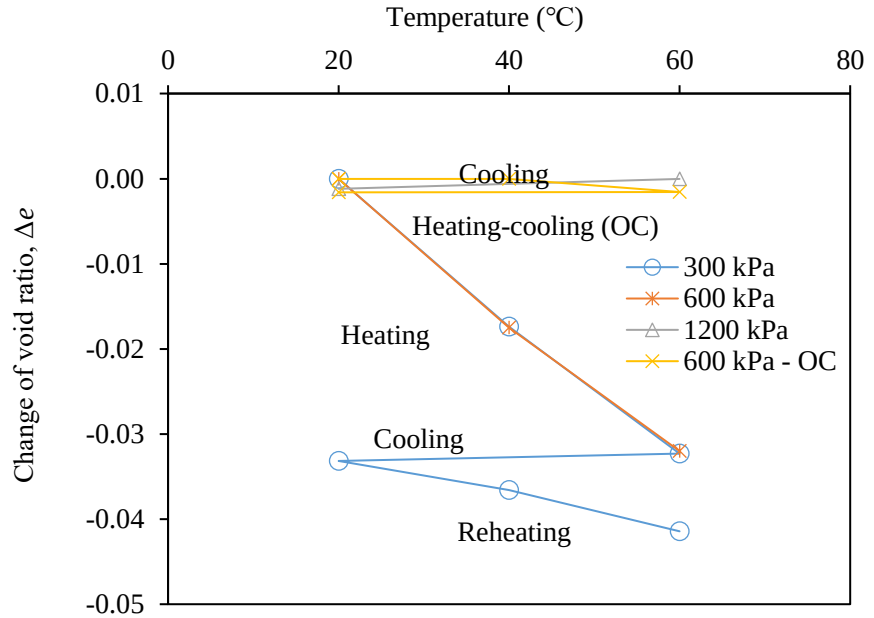

(b)

Fig. 8 Thermally induced changes of void ratio at 24 hours under different vertical effective stress: (a) intact HKMD and (b) reconstituted HKMD

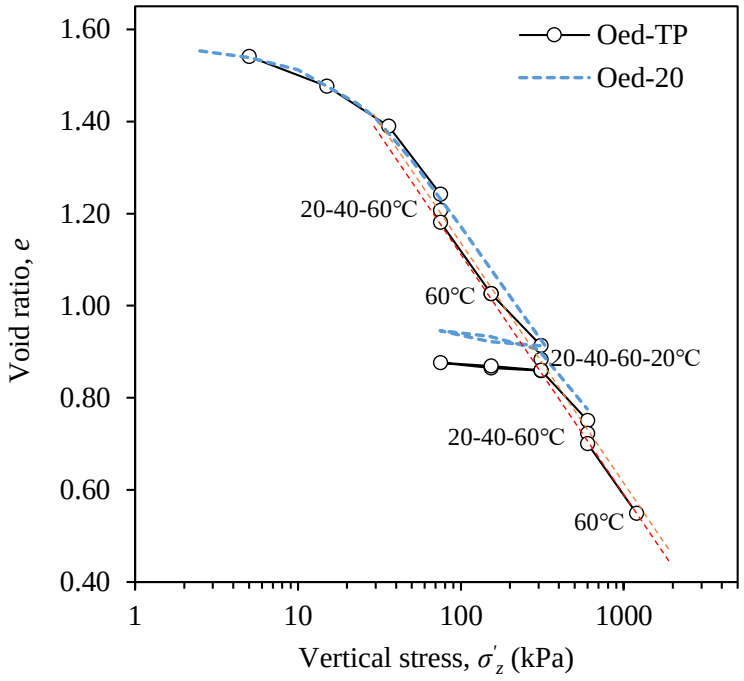

(a)

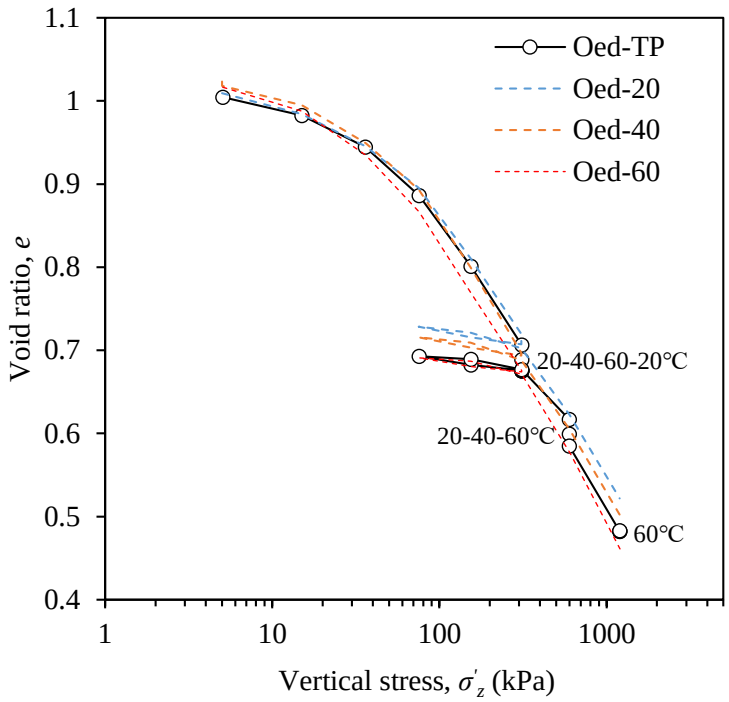

(b)

Fig. 9 1-D compression curves of reconstituted HKMD under step-changed temperatures: (a) intact HKMD and (b) reconstituted HKMD

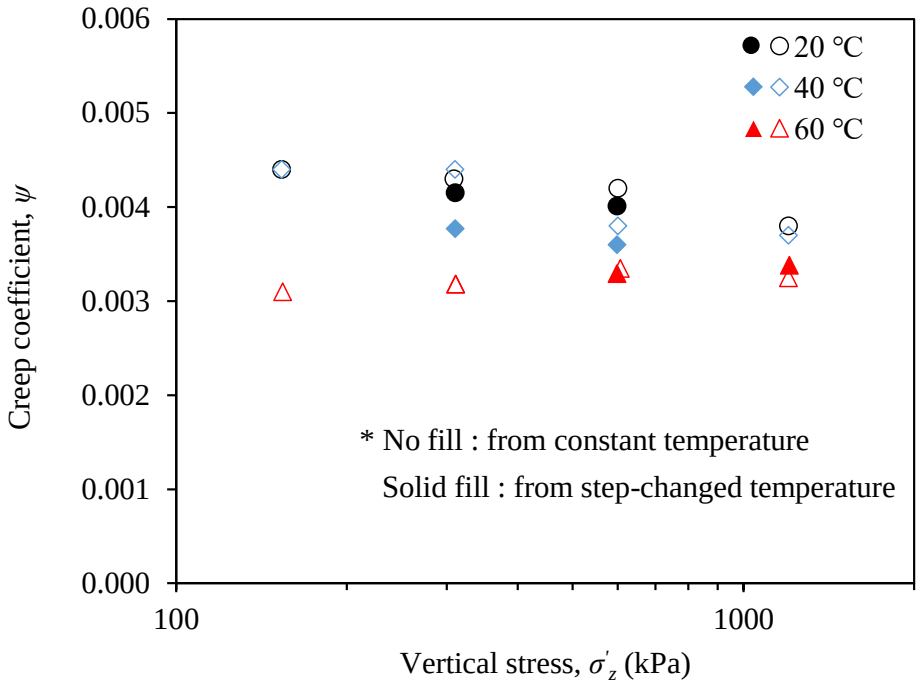

Fig. 10 Creep coefficient of reconstituted HKMD from oedometer tests under different temperature conditions

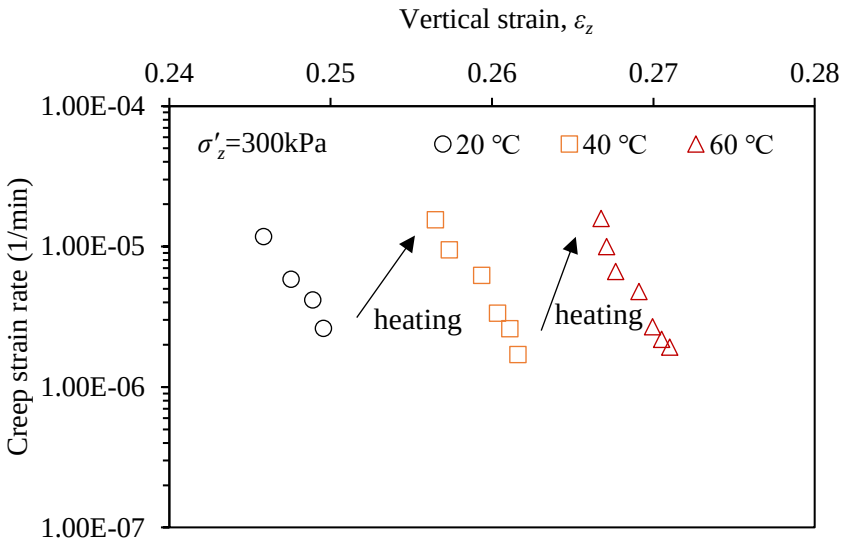

(a)

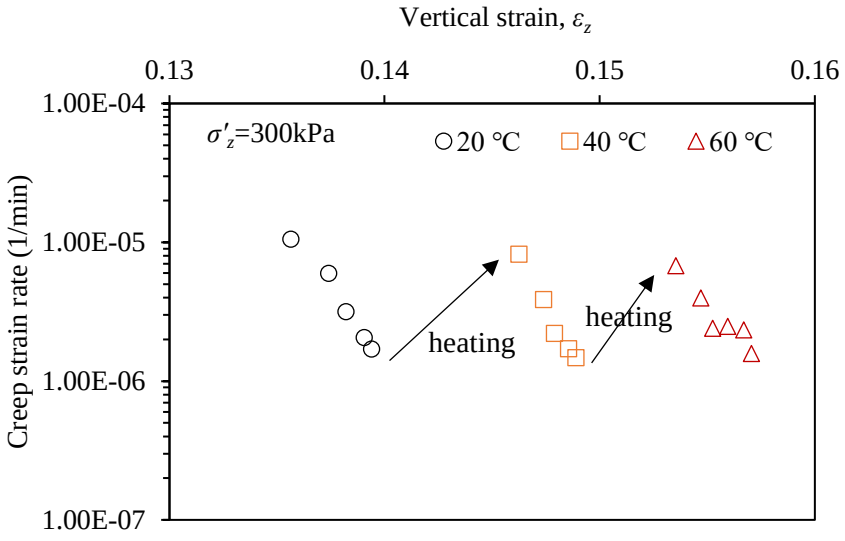

(b)

Fig. 11 Representative $\ln \dot{\varepsilon}_z^{vp} - \varepsilon_z$ curves under changes of temperature: (a) intact HKMD and (b) reconstituted HKMD

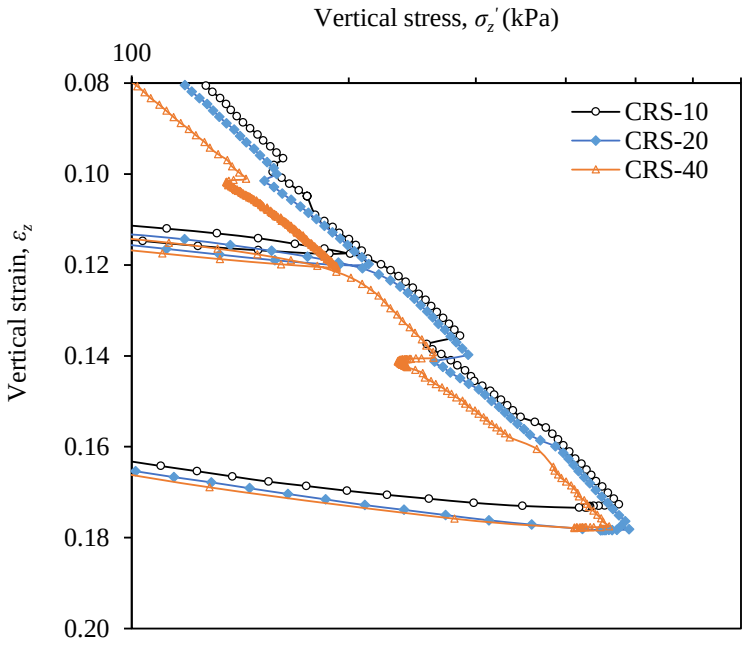

(a)

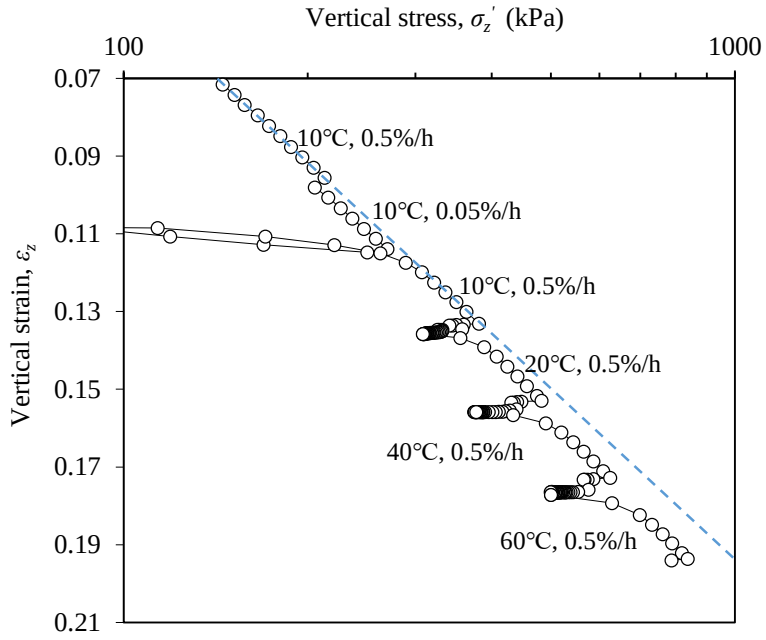

(b)

Fig. 12 1-D compression curves of reconstituted HKMD from CRS tests: (a) under constant temperature and (b) under step-changed temperature

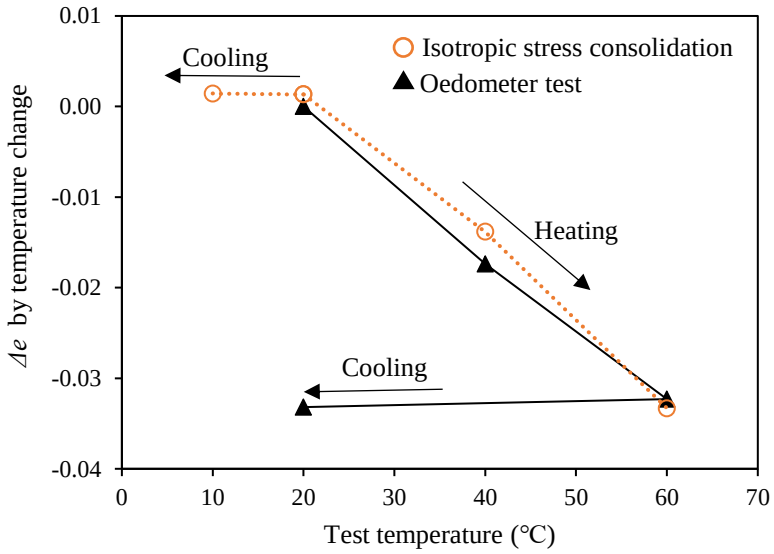

Fig. 13 Thermally induced changes of void ratio under different temperatures in isotropic consolidation tests

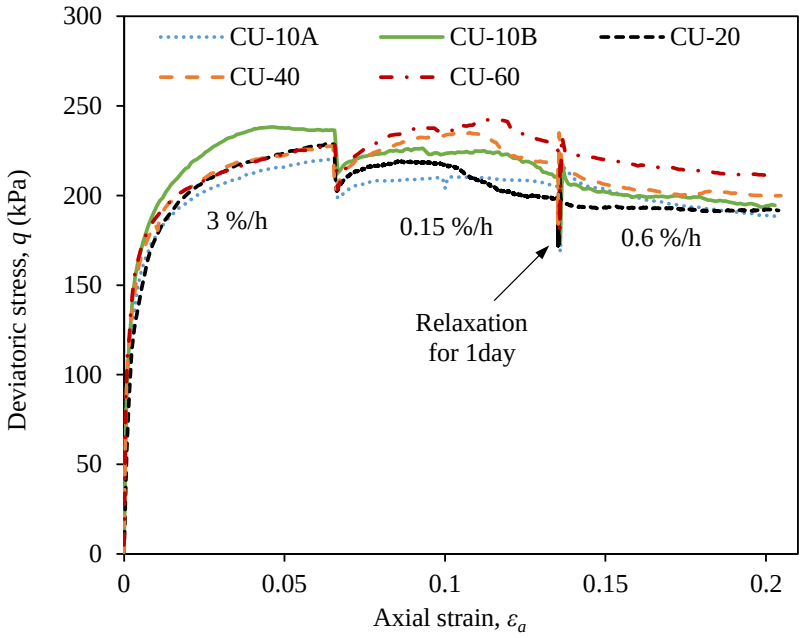
CU-10A
CU-10B
CU-20
CU-40
CU-60
Deviatoric stress, q (kPa)
300
250
200
150
100
50
0
3 %/h
0.15 %/h
0.6 %/h
Relaxation
for 1day
0
0.05
0.1
0.15
0.2
Axial strain, ε_a

(a)

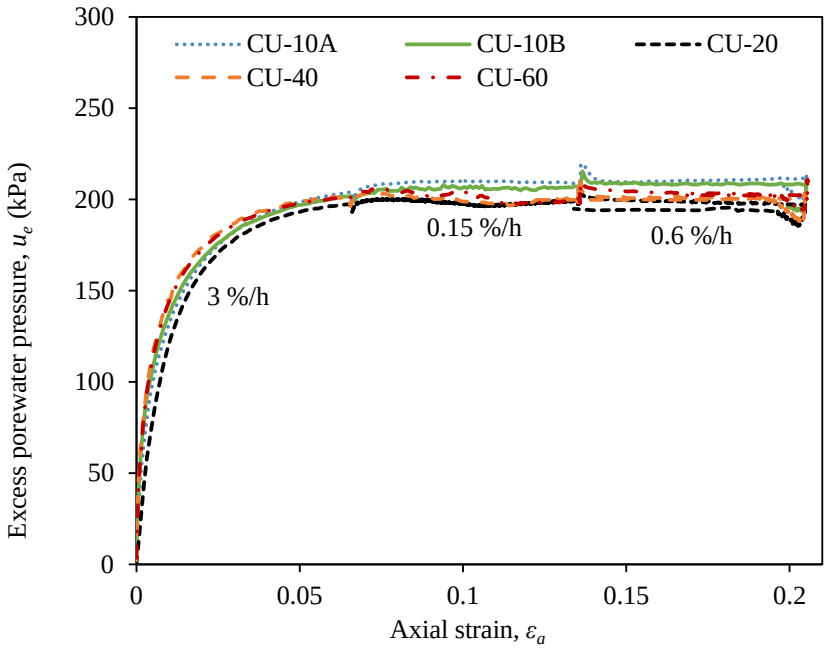
CU-10A
CU-10B
CU-20
CU-40
CU-60
Excess porewater pressure, u_e (kPa)
300
250
200
150
100
50
0
0.15 %/h
0.6 %/h
3 %/h
0
0.05
0.1
0.15
0.2
Axial strain, ε_a

(b)

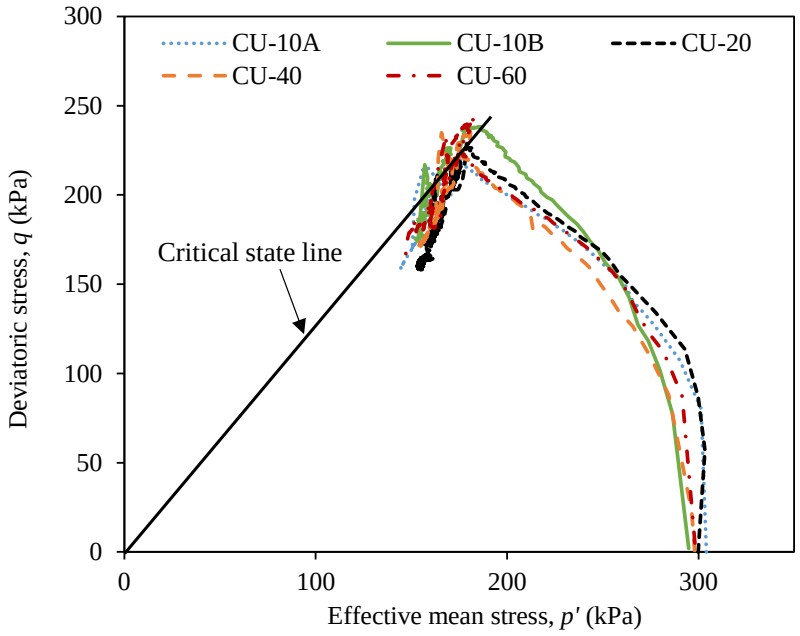

(c)

Fig. 14 Results of the consolidated undrained compression tests under different constant temperatures: (a) deviatoric stress-strain; (b) excess porewater pressure; and (c) effective stress path

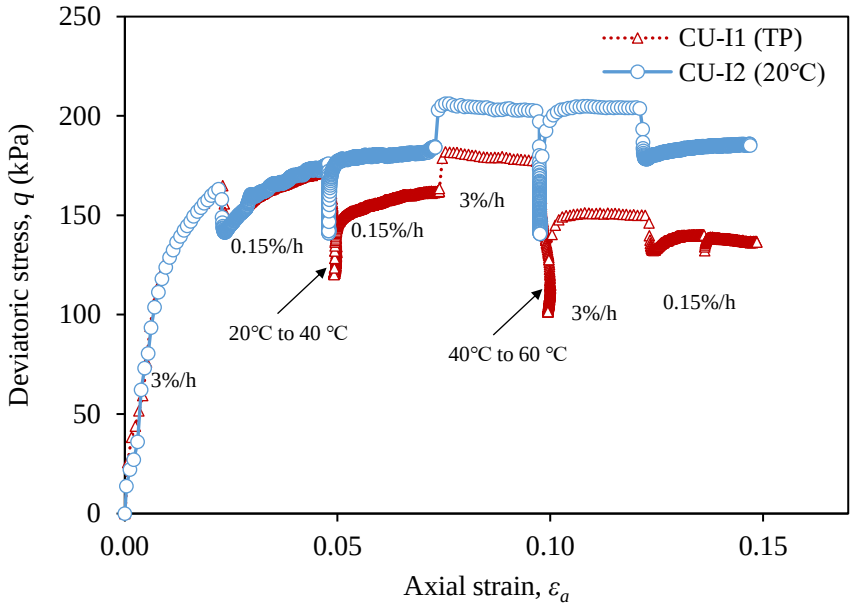
CU-I1 (TP)
CU-I2 (20°C)
Deviatoric stress, q (kPa)
Axial strain, ε_a
250
200
150
100
50
0
0.00
0.05
0.10
0.15
3%/h
0.15%/h
0.15%/h
3%/h
20°C to 40 °C
40°C to 60 °C
3%/h
0.15%/h

(a)

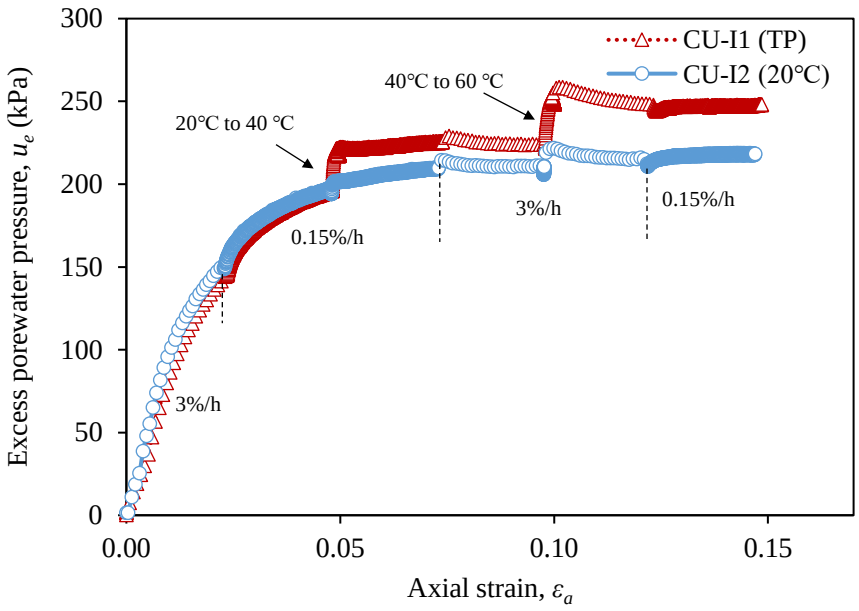
CU-I1 (TP)
CU-I2 (20°C)
Excess porewater pressure, u_e (kPa)
Axial strain, ε_a
300
250
200
150
100
50
0
0.00
0.05
0.10
0.15
40°C to 60 °C
20°C to 40 °C
3%/h
0.15%/h
0.15%/h
3%/h

(b)

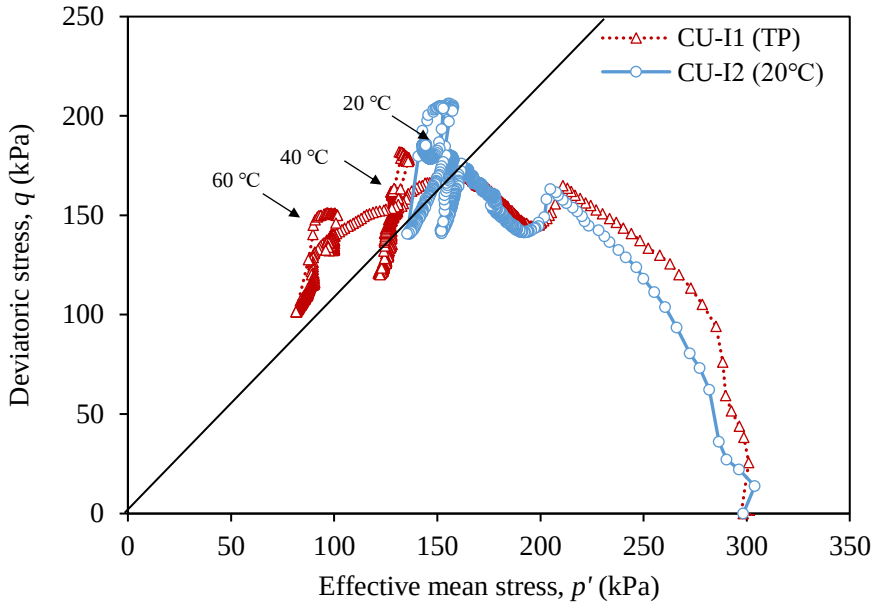

(c)

Fig. 15 Results of the consolidated undrained compression tests on intact HKMD under step-changed temperatures: (a) deviatoric stress-strain; (b) excess porewater pressure; and (c) effective stress path

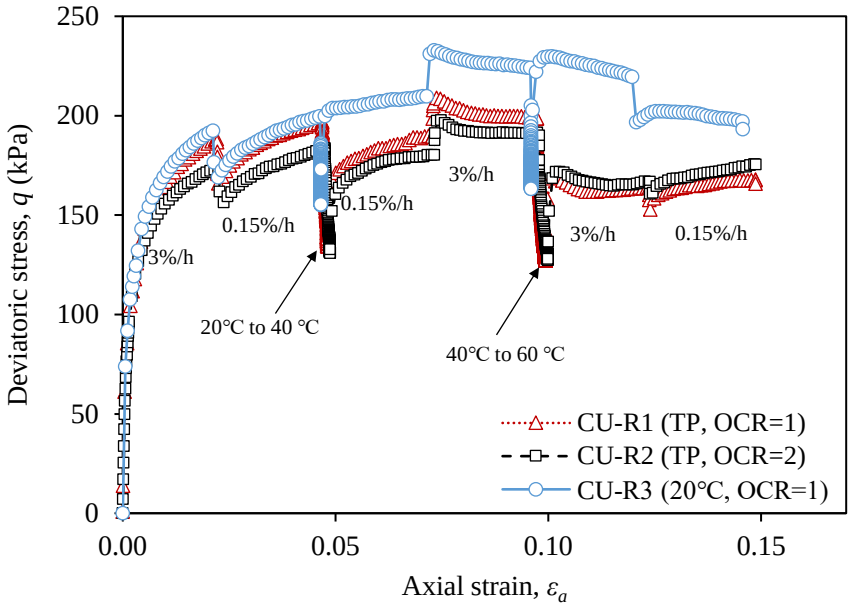
Deviatoric stress, q (kPa)
250
200
150
100
50
0
0.00
0.05
0.10
0.15
Axial strain, ε_a
3%/h
0.15%/h
0.15%/h
3%/h
3%/h
0.15%/h
20℃ to 40 ℃
40℃ to 60 ℃
CU-R1 (TP, OCR=1)
CU-R2 (TP, OCR=2)
CU-R3 (20℃, OCR=1)

(a)

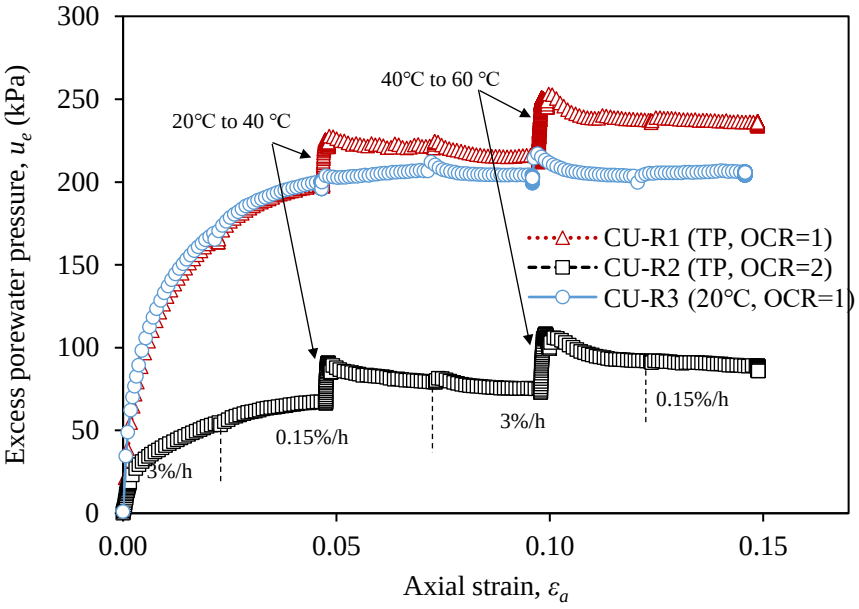
Excess porewater pressure, u_e (kPa)
300
250
200
150
100
50
0
0.00
0.05
0.10
0.15
Axial strain, ε_a
20℃ to 40 ℃
40℃ to 60 ℃
3%/h
0.15%/h
3%/h
0.15%/h
CU-R1 (TP, OCR=1)
CU-R2 (TP, OCR=2)
CU-R3 (20℃, OCR=1)

(b)

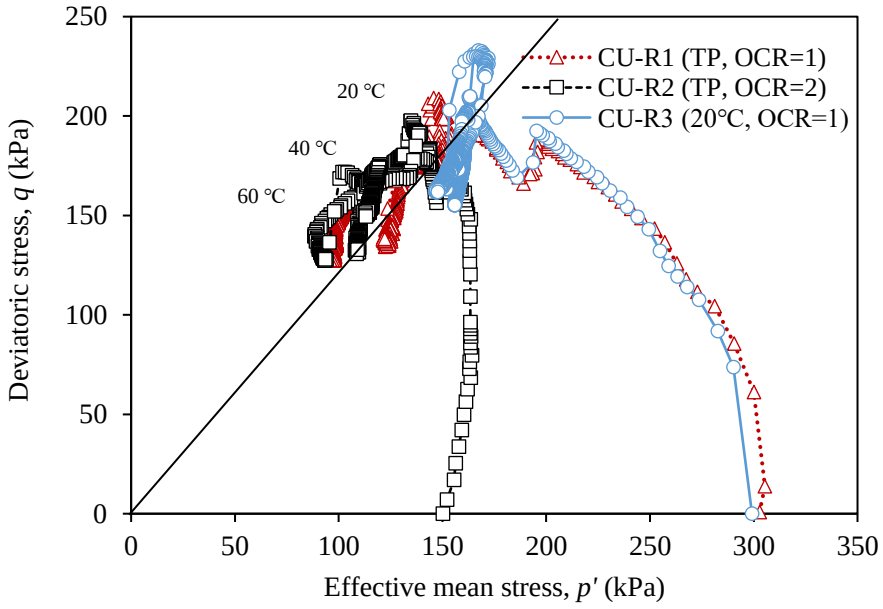

(c)

Fig. 16 Results of the consolidated undrained compression tests on reconstituted HKMD under step-changed temperatures: (a) deviatoric stress-strain; (b) excess porewater pressure; and (c) effective stress path

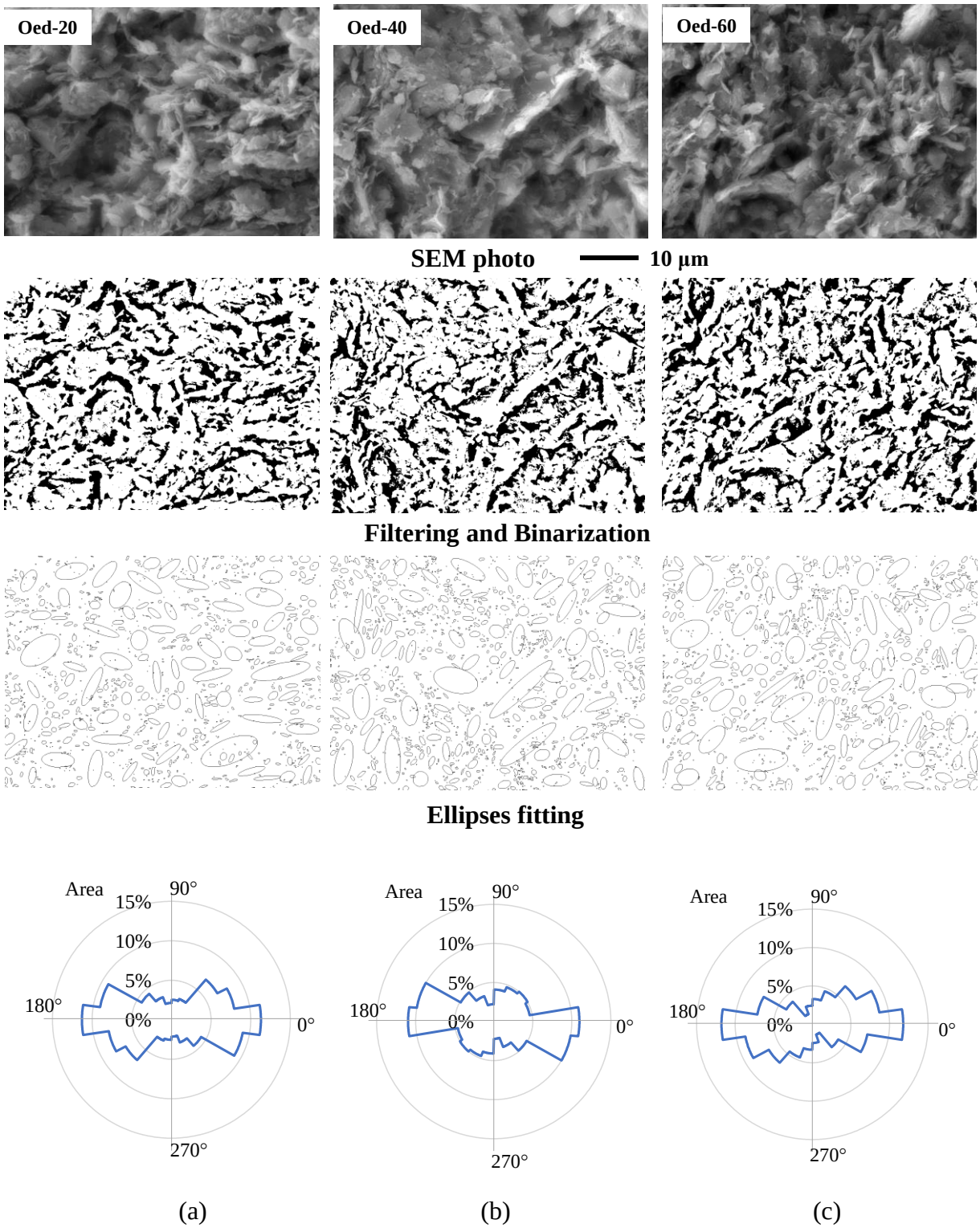

Fig. 17 Analysis of pores orientation and soil fabric of (a) Oed-20, (b) Oed-40, and (c) Oed-60 from SEM under 5,000 x magnification

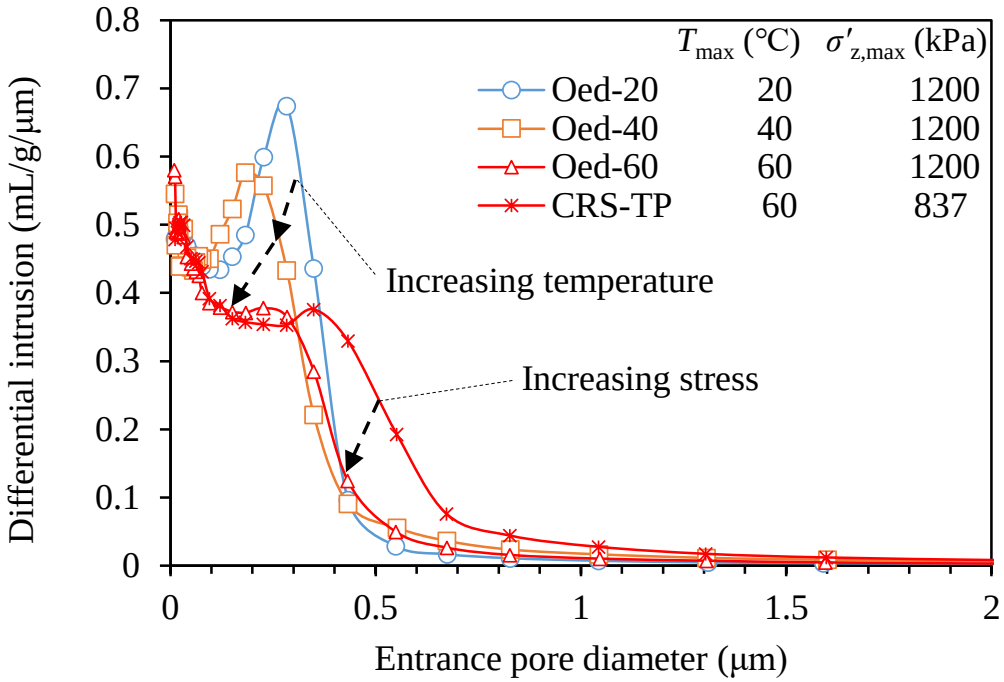

Fig. 18 Distribution of pore size of HKMD from MIP tests

Table 1. Basic physical properties of HKMD

Specific gravity, G_s	Liquid limit, LL	Plastic limit, PL	Plasticity index, PI
2.612	49	31	18

Table 2. Design of the temperature-controlled oedometer tests

Vertical stress (kPa)	Temperature (°C)				
	Intact HKMD	Reconstituted HKMD			
	Oed-TP	Oed-TP	Oed-20	Oed-40	Oed-60
5	20	20	20	40	60
15	20	20			
36	20	20			
75	20→40→60	20			
150	60→20	20			
300	20→40→60→20	20→40→60→20			
150→75→150→300	20	20			
600	20→40→60	20→40→60			
1200	60→20	60→20			
600	20→40→60→20	20→40→60→20			

Table 3. Design of the temperature-controlled CRS tests

Strain stage	Loading rate (temperature)	
	CRS-10, CRS-20, CRS-40	CRS-TP
0~10%	0.5%/h	0.5%/h (10°C)
10~12%	0.05%/h	0.05%/h (10°C)
12~11%	-0.5%/h	-0.5%/h (10°C)
11~14%	0.5%/h	0.5%/h (10°C)
14%	-	Relaxation→heating→relaxation
14~16%	0.01%/h	0.5%/h (20°C)
16%	-	Relaxation→heating→relaxation
16~18%	0.05%/h	0.5%/h (40°C)
18%	-	Relaxation→heating→relaxation
18%-20%	-	0.5%/h (60°C)
20%	-	Relaxation→cooling→relaxation

Table 4. Design of the temperature-controlled consolidated undrained triaxial tests

Test No.	Consolidation temperature	Undrained shearing procedure	Sample type	Consolidation pressure
CU-10A	10°C	3 %/h → 0.15 %/h → Relaxation → 0.6 %/h→ Relaxation	Reconstituted HKMD (R)	300 kPa (OCR=1)
CU-10B	20°C → 10°C			
CU-20	20°C			
CU-40	20°C → 40°C			
CU-60	20°C → 60°C			
CU-R1	20°C	3 %/h → 0.15 %/h → (20°C to 40°C) → 0.15 %/h → 3 %/h → (40°C to 60°C) → 3 %/h → 0.15 %/h		300 kPa → 150 kPa (OCR=2)
CU-R2				
CU-I1			Intact HKMD (I)	300 kPa (OCR=1)
CU-I2		3 %/h → 0.15 %/h → relaxation → 0.15 %/h → 3 %/h → relaxation → 3 %/h → 0.15 %/h		
CU-R3			Reconstituted HKMD (R)	

Table 5. Compression indices and yielding stress of reconstituted HKMD under different temperatures from constant temperature oedometer tests

Temperature (°C)	20	40	60
Normal compression index, λ	0.141	0.144	0.141
Recompression index, κ	0.014	0.013	0.013
Yielding stress, σ'_{zp} (kPa)	55	43	35